

AMBIENT ENERGY HARVESTING BY ZnO
THIN FILM

YIT PEI SHIAN

BACHELOR OF APPLIED SCIENCE (HONOURS)
MATERIAL TECHNOLOGY

UNIVERSITI MALAYSIA PAHANG

UNIVERSITI MALAYSIA PAHANG

DECLARATION OF THESIS AND COPYRIGHT

Author's full name : Yit Pei Shian

Date of birth : 20 October 1993

Title : Ambient Energy Harvesting By ZnO Thin Film

Academic Session : Semester I 2016/2017

I declare that this thesis is classified as:

CONFIDENTIAL (Contains confidential information under the Official Secret Act 1972)

RESTRICTED (Contains restricted information as specified by the organization where research was done)

OPEN ACCESS I agree that my thesis to be published as online open access (Full text)

I acknowledge that Universiti Malaysia Pahang reserve the right as follows:

1.4.1 The Thesis is the Property of Universiti Malaysia Pahang

1.4.2 The Library of Universiti Malaysia Pahang has the right to make copies for the purpose of research only.

1.4.3 The Library has the right to make copies of the thesis for academic exchange.

Certified By:

(Student's Signature)

Yit Pei Shian
931020-01-5900
Date:

(Supervisor's Signature)

Assoc. Prof. Dr. Agus Geter Edy
Sutjipto
Date:

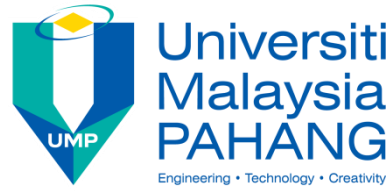
AMBIENT ENERGY HARVESTING BY ZNO THIN FILM

YIT PEI SHIAN

Thesis submitted in fulfillment of the requirements
for the award of the degree of
Bachelor of Applied Science (Hons) Material Technology

Faculty of Industrial Sciences & Technology
UNIVERSITI MALAYSIA PAHANG

DECEMBER 2016

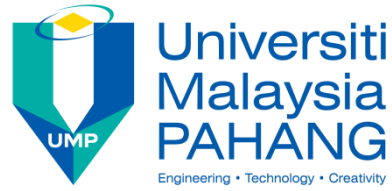


SUPERVISORS' DECLARATION

I hereby declare that I have checked this thesis and in my opinion, this thesis is adequate in terms of scope and quality for the award of the degree of Bachelor of Applied Science (Honor) Material Technology.

(Supervisor's Signature)

Name of Supervisor : ASSOC. PROF. DR. AGUS GETER EDY
SUTJIPTO
Position : ASSOCIATE PROFESSOR
Date :



STUDENT'S DECLARATION

I hereby declare that the work in this thesis is my original work except for quotations and citation which have been duly acknowledged. I also declare that it has not been previously or concurrently submitted for any other degree at Universiti Malaysia Pahang or any other institutions.

(Student's Signature)

Name : YIT PEI SHIAN

ID Number : SC13007

Date :

DEDICATION

Dedicated to my parents, my supervisor, Assoc. Prof. Dr. Agus Geter
Sutjipto, lab assistances and my fellow friends.

ACKNOWLEDGEMENTS

First of all, I would like to express my sincere appreciation to my project supervisor, Dr. Agus Geter Edy Sutjipto for his continuous encouragement, consistent support, insightful comments, advice and exceptional guidance. I would like to express my grateful to him for his tolerance and patience to spend a lot of time to answer my questions and give practical suggestions during this period.

Besides that, I would like to express my appreciation to laboratory assistant of Faculty Science and Industrial Technology, UMP, who assisted me throughout my journey of laboratory work in order to success the project. Not to be forgotten, my lovely coursemate who accompanied me whenever I need.

I would also like to express my gratitude to all lecturers who had guided me along the journey. Lastly, many special thanks go to my parents for their love and endless support.

ABSTRACT

This thesis deals with ambient energy harvesting using zinc oxide thin film. The objectives of this thesis are to prove the ZnO film as a piezoelectric material can produce electric when vibration is applied and determine its optimal voltage. This thesis describes the sol gel spin coating technique to fabricate zinc oxide thin film. Zinc acetate dehydrate, absolute ethanol and diethanolamine were used to act as sol gel precursor. Sol gel was coated on glass slide which wrapped by aluminum foil. The thin film was formed after preheating and annealing. The thin film was characterized by X-ray diffraction (XRD), Field Emission Scanning Electron Microscopy (FESEM), Photoluminescence Spectroscopy (PL) and Ultraviolet-visible Spectroscopy (UV-Vis) as well as analyzed using vibration technique. From XRD results, the films were preferentially diffracted at around 65° which corresponding to (1 1 2) diffraction phase. From FESEM results, it was observed that when the spin speed was increased at same annealing temperature, the thickness was also decreased. When the annealing temperature was increased at same spin speed, both grain size and thickness were increased. From the PL results, there was only film with spin speed of 2000 rpm and annealing temperature of 300°C had slightly left wavelength which was 380 nm. Annealing temperature would affect only the intensity of PL wavelength. From the results of UV-Vis, it was observed that when the spin speed was increased at same annealing temperature, the band gap was decreased. When the annealing temperature was increased at same spin speed, the band gap was decreased. Piezoelectric test had proven the ZnO film could produce electricity. The maximum voltage (20.7 mV) was produced by the ZnO film with spin speed of 2000 rpm and annealing temperature of 300°C .

TRANSLATION OF ABSTRACT

Tesis ini berkaitan dengan menuaikan tenaga ambien dengan menggunakan filem zink oksida. Objektif projek ini adalah untuk membuktikan filem ZnO sebagai bahan piezoelektrik boleh menghasilkan elektrik apabila dikena dengan getaran dan menentukan voltan optimum. Tesis ini menerangkan teknik lapisan gel putaran untuk mereka-reka filem zink oksida. Kering zink oksida, etanol mutlak dan dietanolamine telah digunakan dalam tesis ini untuk menjadi sebagai pelopor. Sol gel telah disalut pada slaid kaca yang dibalut dengan aluminium. Filem akan dibentuk selepas pra-pemanasan dan suhu penyepuhlindapan. Filem telah dicirikan oleh pembelauan sinar-X, mikroskop elektron pengimbas pancaran medan (FESEM), spektroskopi fotoluminisen (PL) dan spektroskopi ultra lumbayung-nampak (UV-Vis) serta dianalisis dengan teknik getaran. Daripada keputusan XRD, filem telah dibelaukan pada 65° yang sepadan dengan (1 1 2) fasa. Daripada keputusan FESEM, ketebalan telah menurun apabila meningkatkan kelajuan putaran pada suhu penyepuhlindapan yang sama. Saiz partikel dan ketebalan telah meningkat apabila meningkatkan suhu penyepuhlindapan pada kelajuan putaran yang sama. Daripada keputusan PL, hanya filem dengan kelajuan putaran dengan 2000 rpm dan suhu penyepuhlindapan dengan 300°C telah meninggalkan panjang gelombang daripada yang lain, iaitu 380 nm. Suhu penyepuhlindapan akan menjejaskan hanya intensiti PL. Daripada hasil UV-Vis, apabila kelajuan putaran telah meningkat pada suhu penyepuhlindapan sama, nilai tenaga jurang telah berkurang. Apabila suhu penyepuhlindapan telah meningkat pada kelajuan putaran sama, nilai tenaga jurang ini telah berkurang. Ujian piezoelektrik telah membuktikan filem ZnO yang boleh menghasilkan tenaga elektrik. Voltan maksimum (20.7 mV) telah dihasilkan oleh filem ZnO dengan kelajuan putaran dengan 2000 rpm dan suhu penyepuhlindapan dengan 300°C .

TABLE OF CONTENTS

	Page
DECLARATION OF THESIS AND COPYRIGHT	i
SUPERVISORS' DECLARATION	
STUDENT'S DECLARATION	
DEDICATION	ii
ACKNOWLEDGEMENTS	iii
ABSTRACT	iv
TRANSLATION OF ABSTRACT	v
TABLE OF CONTENTS	vi
LIST OF TABLES	ix
LIST OF FIGURES	x
LIST OF SYMBOLS	xiii
LIST OF ABBREVIATIONS	xiv
CHAPTER 1 INTRODUCTION	
1.1 Introduction	1
1.2 Problem Statement	3
1.3 Objectives of Research	4
1.4 Statement Of Contribution	4
CHAPTER 2 LITERATURE REVIEW	
2.1 Introduction of Piezoelectric Effect	6
2.2 Piezoelectric Material, ZnO	7
2.3 Sol Gel Deposition	9
2.4 Precursor Material	10
2.5 Solvent, Absolute Ethanol	12
2.6 Thin Film Preparation Method	13
2.7 Annealing Effect	14
2.8 Energy Harvesting Test	15

2.9	Application Of Piezoelectric	15
-----	------------------------------	----

CHAPTER 3 MATERIALS AND METHODS

3.1	Introduction	18
3.2	Material Synthesis Methods	19
3.2.1	Material and Apparatus	19
3.2.2	Preparation of Precursor Solution	20
3.3	Fabrication Of Zno Thin Film	21
3.3.1	Spin speed	21
3.3.2	Heat Treatment	23
3.4	Characterization Of Zno Thin Film	23
3.4.1	X-ray Diffraction (XRD)	24
3.4.2	Field Emission Scanning Electron Microscopy (FESEM)	24
3.4.3	UV-VIS Spectroscopy	25
3.4.4	Photoluminescence Spectroscopy	25
3.5	Piezoelectric Test	26

CHAPTER 4 RESULTS AND DISCUSSION

4.1	Introduction	27
4.2	Synthesis and Characterization of ZnO Thin Film	28
4.2.1	X-Ray Diffraction Analysis	28
4.2.2	Morphology Analysis	36
4.2.3	Photoluminescence	49
4.2.4	UV-Vis Analysis	50
4.3	Piezoelectric Test	54

CHAPTER 5 CONCLUSION AND RECOMMENDATION

5.1	Conclusion	56
-----	------------	----

5.2 Recommendations	56
REFERENCES	58
APPENDICES	62

LIST OF TABLES

Table	Title	Page
2.1	Sol gel undoped ZnO thin film methods	11
4.1	(h k l) plane, d-spacing and crystalline size for the ZnO thin films with different spin speed and annealing temperature	35
4.2	Nanoparticle size of ZnO films with different spin speed and annealing temperature	36
4.3	Thickness of ZnO thin film with different spin speed and annealing temperature	48
4.4	Energy band gap of UV emission peak at different spin speed and annealing temperature of ZnO thin film	53
4.5	Voltage that could be produced by each films	55

LIST OF FIGURES

Figure	Title	Page
2.1	An illustration of piezoelectric phenomenon (a) direct piezoelectric effect and (b) neutral state of piezoelectric material	7
2.2	Piezopotential in wurtzite crystal	8
2.3	Steps of preparation of (a) thin films and (b) powders by sol gel process	9
2.4	Thin film preparation techniques	13
2.5	XRD pattern ZnO thin film by spin coating at different annealing temperature	15
2.6	Shoe Power Generator	16
3.1	Flow chart of methodology research	19
3.2	Flow chart of preparation of precursor solution	20
3.3	ZnAc dissolved in absolute ethanol on hot plate	21
3.4	Spin coating instrument	22
3.5	ZnO film formed with spin speed of 2000 rpm and annealing temperature of 300 °C	22
3.6	List of methods used to characterize the ZnO films	23
3.7	FESEM instrument (a) Zeiss EVO 50 SEM and (b) Baltec-SCD 005 Sputter Coater	24
3.8	Connection of copper wire with two electrodes	26
3.9	Schematic diagram of piezoelectric testing	26
4.1	XRD pattern of ZnO thin film with spin speed of 1000 rpm and annealing temperature 300 °C	29
4.2	XRD pattern of ZnO thin film with spin speed of 1500 rpm and annealing temperature 300 °C	30
4.3	XRD pattern of ZnO thin film with spin speed of 2000 rpm and annealing temperature 300 °C	31
4.4	XRD pattern of ZnO thin film with spin speed of 1500 rpm and annealing temperature 400 °C	32
4.5	XRD pattern of ZnO thin film with spin speed of 1500 rpm and annealing temperature 500 °C	33

4.6	XRD spectrum of each film	34
4.7	XRD spectrum of ZnO film with spin speed of 1500 rpm and annealing temperature of 180 °C	35
4.8	Surface morphology of ZnO thin with spin speed of 1000 rpm and annealed at 300 °C with different magnification (a) 5 kx, (b) 50 kx, (c) 150 kx (d) 150 kx with measurement	37
4.9	Surface morphology of ZnO thin with spin speed of 1500 rpm and annealed at 300 °C with different magnification (a) 5 kx, (b) 50 kx, (c) 150 kx (d) 150 kx with measurement	38
4.10	Surface morphology of ZnO thin with spin speed of 2000 rpm and annealed at 300 °C with different magnification (a) 5 kx, (b) 50 kx, (c) 150 kx (d) 150 kx with measurement	39
4.11	Surface morphology of ZnO thin with spin speed of 1500 rpm and annealed at 400 °C with different magnification (a) 5 kx, (b) 50 kx, (c) 150 kx (d) 150 kx with measurement	40
4.12	Surface morphology of ZnO thin with spin speed of 1500 rpm and annealed at 500 °C with different magnification (a) 5 kx, (b) 50 kx, (c) 150 kx (d) 150 kx with measurement	41
4.13	Cross section of ZnO film on Al substrate with spin speed of 1000 rpm and annealed at 300 °C	42
4.14	Cross section of ZnO film with spin speed of 1000 rpm and annealed at 300 °C with different magnification at several parts of sample	43
4.15	Cross section of ZnO film with spin speed of 1500 rpm and annealed at 300 °C with different magnification at several parts of sample	44
4.16	Cross section of ZnO film with spin speed of 2000 rpm and annealed at 300 °C with different magnification at several parts of sample	45
4.17	Cross section of ZnO film with spin speed of 1500 rpm and annealed at 400 °C with different magnification at several parts of sample	46
4.18	Cross section of ZnO film with spin speed of 1500 rpm and annealed at 500 °C with different magnification at several parts of sample	47
4.19	Surface morphology of ZnO film with spin speed of 1500 rpm and annealing temperature of 180 °C	48
4.20	PL spectrum of ZnO thin film with different spin speed and annealing temperature	49
4.21	UV spectrum of ZnO film with spin speed of 1000 rpm and annealing temperature of 300 °C	51
4.22	UV spectrum of ZnO film with spin speed of 1500 rpm and annealing temperature of 300 °C	51

4.23	UV spectrum of ZnO film with spin speed of 2000 rpm and annealing temperature of 300 °C	52
4.24	UV spectrum of ZnO film with spin speed of 1500 rpm and annealing temperature of 400 °C	52
4.25	UV spectrum of ZnO film with spin speed of 1500 rpm and annealing temperature of 500 °C	53
4.26	ZnO film with spin speed of 1500 rpm and annealing temperature of 180 °C	54
4.27	Voltage produced by each film	55

LIST OF SYMBOLS

~	approximately
%	percent
λ	wavelength
2θ	Bragg angle
$^{\circ}\text{C}$	degree celcius
\AA	angstrom (10^{-10})
h	hour
t	time
s	seconds
rpm	rotation per minutes
mol	no of mole
min	minutes
ml	milliliter
cm	centimeter
kV	kilovolt
mA	milliampere
nm	nanometer
kHz	kilohertz

LIST OF ABBREVIATIONS

FESEM	Field Emission Scanning Electron Microscopy
PL	Photoluminescence
UV-Vis	Ultraviolet-Visible Microscopy
XRD	X-ray diffraction
ZnO	Zinc Oxide
Al	Aluminum
ZnAc	Zinc Acetate Dehydrate
DEA	Diethanolamine
A. EtOH	Absolute Ethanol
MeOH	Methanol
EtOH	Ethanol
PrOH	Propanol
NaOH	Sodium Hydroxide
MEA	Monoethanolamine
a-SiO ₂	amorphous-Silicon Dioxide

CHAPTER 1

INTRODUCTION

1.1 Introduction

Electricity is generated from non-renewable natural sources such as fossil fuel, coal, natural gas, and petroleum. The electricity is being used in many fields such as automotive, health care and communication devices. For example, for application in medical science, nano-devices and wireless sensors require electricity for their power sources. To use in powering the wireless nano-devices, the regular energy source, battery is facing the limitation due to its big size, heavy weight and short operation lifetime (Prashanthi, et al., 2013; Kumar & Kim, 2012). Even though battery has high capacitance, it is not energy efficient. Most of the energy input has been lost as heat, light, sound or vibration. Battery has low power density. In addition, battery is not environmental friendly power resource. Therefore, it has drawn the emergence of research in alternative energy sources to fulfill the needs of wireless sensing problem.

Moreover, these non-renewable natural sources have caused the depletion of ozone layer and global warming. To maintain sustainably development for human civilization, many researches are now focusing on searching renewable alternative way to solve the shortage of natural resources and reduce the pollution (Aricò, Bruce, Scrosati, Tarascon, & Schalkwijk, 2005).

To break through the insufficiency of traditional power sources and achieve green energy technology, energy harvesting has drawn attention from scientist. Energy harvesting is a device that can convert the unused ambient energy to electricity. The

type of energy harvesting depends on the type of energy and applications. Energy harvesting is distinguished as radiant energy harvesting, mechanical energy harvesting, thermal energy harvesting, vibration energy harvesting and others. Energy harvesting is mostly used for low-powered electronic applications, such as wireless devices. This technologies use material at micro- or nano- scale to charge wireless devices and wireless sensor networks.

There are many benefits of energy harvesting. One of the benefits is to reduce usage of battery power. Device with low-powered can be charged by energy harvester and rely on internal energy storage rather than rely on battery power. Self-powered wireless sensor is easy to install. Therefore, it can reduce installation cost. Energy harvesting also can reduce maintenance cost as there is not necessary to replace battery. Self- powered device can be used in long term as long as the ambient energy is available. Energy harvester also reduces environmental impact(Chen, He, & Sun, 2014; Wong & Dahari, 2015).

Among these few types of energy harvesting, vibration energy harvester has drawn more attention in the world as it is available almost everywhere at all times. It can be used in many fields such as implanted devices, electronic devices, mobile devices and wireless sensor devices (Khaligh, Zeng, & Zheng, 2010). There are three ways to generate electrical energy from vibration energy which are electromagnetic, piezoelectric and electrostatic. It is hard to fabricate the circuit of electromagnetic as it has low voltage and cannot produce high current. Electrostatic cannot be used in practical as it requires external voltage sources (Shang, Li, Wen, & Zhao, 2013). Therefore, piezoelectric vibration harvester has been focused more.

The piezoelectric effect converts mechanical energy (vibration, air flow and human physical motion (Kumar & Kim, 2012)) into electrical energy. In 1880, Curie and his brother discovered the piezoelectric effect. During World War I, the application of piezoelectric effect in solar device had been launched. After that, new applications such as microphones, accelerometers, actuators and ultrasonic motors were developed (Spies, Pollak, & Mateu, 2015). Nuffer and Bein proposed that piezoelectric energy harvester acts as a knock sensor to detect irregular combustion in transportation industry

(Nuffer & Bein, 2006). It has become common and easy to find the application of piezoelectric material.

Thin film technology has great potential to produce micro- or nano- scale devices as piezoelectric thin film. Thin film is a 2D nanomaterial which means that two of the dimensions are not confined to the nanoscale. Thin film exists in platelike shape. It offers many benefits in various applications for example, high energy density harvester, high sensitivity but low power sensors and high resolution circuit board. Moreover, compare to bulk piezoelectric materials, piezoelectric thin films are more suitable to be integrated into micromechanical systems (MEMS) or nanoelectromechanical systems (NEMS) (Eom & Trolier-Mckinstry, 2012).

1.2 Problem Statement

There are many novel ideas of renewable energy harvesting application. However, the major challenges faced by developers are to construct an energy harvester that is cheap, efficient and can work all the time especially when the ambient unused energy is absent. From this case, the combination of semiconductor and piezoelectric plays an important role in energy harvesting.

Piezoelectric semiconducting materials (ZnO, AlN, ZnS, GaN) have been used in many fields to generate power. Among these materials, ZnO has been focused more due to its favorable properties (high electron mobility, high power stability and inherent piezoelectric properties).

There are many studies revealed that the characterization and vibration sensing performance of ZnO nanostructures as piezoelectric energy harvester under different annealing temperature, but the energy harvester based on ZnO thin film was rarely reported.

This paper presents the fabrication process of ZnO thin film by spin coating and the measurement of the energy harvester based on ZnO thin film. The characterizations (crystallographic orientation, composition of ZnO, thickness of thin film and the current

output) of ZnO thin film are determined. In this present work, ultrasonic cleaner is used to determine the effect of vibration on the voltage produced from ZnO thin film.

1.3 Objectives of Research

The objectives of this research are stated as below.

1. To fabricate ZnO based thin film by spin coating
2. To characterize ZnO thin film using X-ray Diffraction (XRD), Field Emission Scanning Electron Microscopy (FESEM), photoluminescence and UV-Vis spectroscopy
3. To prove ZnO thin film piezoelectric as vibration energy harvester can produce electric
4. To determine the optimal piezoelectric voltage by varying the temperature and speed during spin coating

1.4 Statement of Contribution

The scopes of study are

1. To synthesis ZnO sol gel
Zinc oxide comes from group II-IV semiconductor which has a wide band gap (3.37eV). The properties of ZnO that made it as the candidate of this study are environmental friendly, low cost, chemical stability towards air and biologically safe. It is able to coat for large area. ZnO sol was prepared by adding with precursor sol of zinc acetate dehydrate in 70 ml of absolute ethanol solution and diethanolamine (DEA).
2. To fabricate ZnO based thin film.
Thin film coating process involves solution preparation, coating and drying. ZnO sol was deposited on an aluminum foil which acts as an electrode by spin coating process. Aluminum foil was being chosen because it is low cost, non-toxic, good electricity, and stable at high temperature. The method of spin coating was used because it is simple and low cost.

3. To analyze the ZnO thin film by using XRD, FESEM, photoluminescence and UV-Vis spectroscopy to examine the surface morphology and physical properties.
4. To investigate the effect of vibration on voltage produced from piezoelectric ZnO thin film.

CHAPTER 2

LITERATURE REVIEW

2.1 Introduction of Piezoelectric Effect

Piezoelectric is derived from Greek word where “piezo” means pressure and “electric” means electricity. Piezoelectric effects characterize into two types, which are direct and indirect. Direct piezoelectric effect means that an electric charge is being generated across the material when a mechanical strain (stress) is applied to the piezoelectric material. Conversely, indirect piezoelectric effect means that a deformation of material happens when an electric field is applied to the piezoelectric material (Nechibvute, Chawanda, & Luhanga, 2012).

The requirement of piezoelectric material is that the atomic arrangement have no center of symmetry. There is only twenty out of thirty-two crystal classes that have piezoelectric effect. The most important piezoelectric material is quartz (SiO_2).

Figure 2.1 shows piezoelectric phenomenon. Piezoelectric material generates current when a pressure is applied as shown in Figure 2.1a. When a pressure is applied on piezoelectric material, polarization occurs and a charged density is generated in crystals of piezoelectric material. One side of crystal has net positive charge and a net negative charge is at opposite site. The polarization establishes an electric field and causes current flow. Polarization will remain as long as the force is applied. The effect is called as direct polarization effect. Polarization will be disappeared and no current flow when the pressure applied is stopped (Vives, 2008). In contrast, mechanical

deformation of piezoelectric material will be occurred when a voltage is applied. The effect is then called as indirect polarization effect.

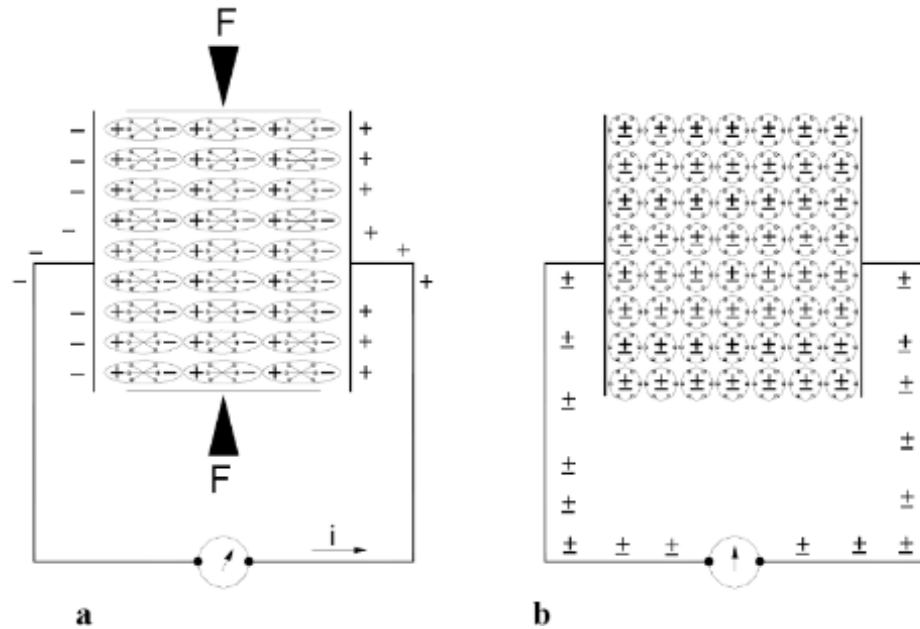


Figure 2. 1. An illustration of piezoelectric phenomenon (a) direct piezoelectric effect and (b) neutral state of piezoelectric material.

Source: Reproduced from (Vives, 2008)

2.2 Piezoelectric Material, ZnO

Zinc oxide (ZnO) comes from group II-IV group semiconductor. It is a transparent conducting oxide. ZnO has a hexagonal wurtzite structure with non centrosymmetric characteristic as shown in Figure 2.2 (a). It possess strong piezoelectric and pyroelectric properties. Besides that, it has a wide band gap which is about 3.37 eV at room temperature. This means that it is suitable to use for short wavelength application such as laser. It also has high exciton binding energy which is about 60 meV so that excitonic emission is efficient at room temperature (Wang, Zhong Lin, 2004).

Zinc oxide, semiconducting material possess piezoelectric characteristic. It generates a small piezoelectric coefficient. It has a preferable highly c-axis oriented with a peak of (002). C-axis preferential thin film is important for piezoelectric devices because along with c-axis, ZnO crystal has the largest coupling constant. This means that, c-axis oriented ZnO film has shorter carrier path in c-axis and hence has lower resistivity. Therefore, it has high mobility of electrons (Yahya, 2011). The lattice parameters of ZnO structure are $a = 0.325$ nm and $c = 0.521$ nm. Zn^{2+} and O^{2-} ions are tetrahedral bonded and it has overlapping at the centers of charge of positive and negative ions (Alias & Mohamad, 2013). When a stress is applied at the top of tetrahedron, a dipole moment will be induced due to the displacement of the charge. The dipole moment will generate a piezopotential and the potential drop will maintain as long as the stress is maintained. When an external cable is connected, piezopotential will drive the flow of electron and induce a voltage (Wang & Wu, 2014).

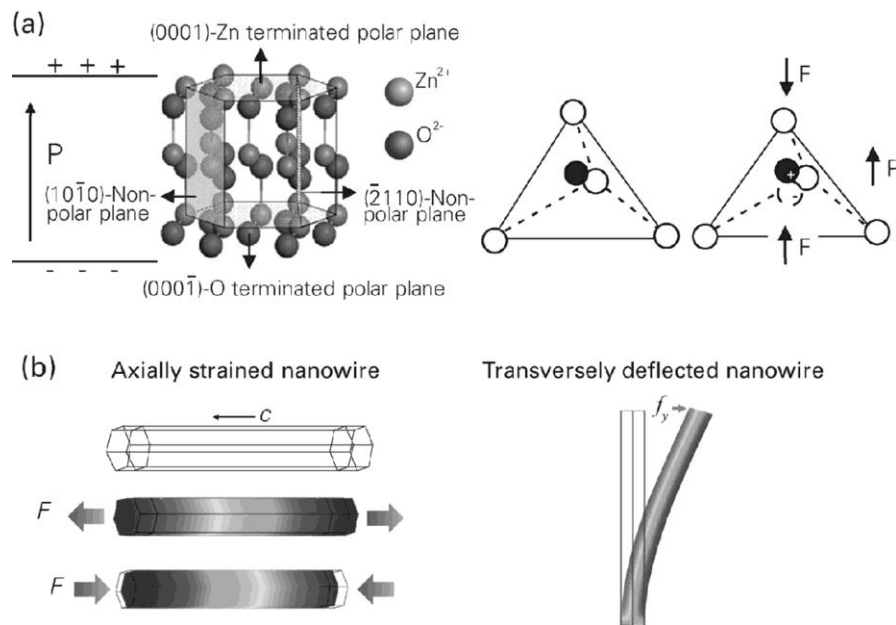


Figure 2.2. Piezopotential in wurtzite crystal.

Source: Reproduced from (Wang & Wu, 2014)

2.3 Sol Gel Deposition

Sol gel is a process to synthesis nanoscale materials. It is used to fabricate metal oxides nanoparticles. Sol gel process is most common method for synthesise ZnO nanoparticles. ZnO thin film can be made by sol-gel processing.

The advantages of sol gel process are controllability of compositions(Nanda & Gupta, 2010), simple, cost effective, inexpensive, non-vacumm and low temperature treatment. Besides that, homogeneity of solution is easily controlled to form a uniform film. (Kondraties, Kink, & Romanov, 2013).

Sol gel process involves transition phase of a liquid sol to a solid gel by hydrolysis and condensation reaction (Znaidi, L., 2010). Figure 2.3 shows the illustration of sol gel process. Sol gel process is generally involves 3 principle steps, which are preparation of precursor solution, deposition of sol on suitable substrate by appropriate technique and heat treatment.

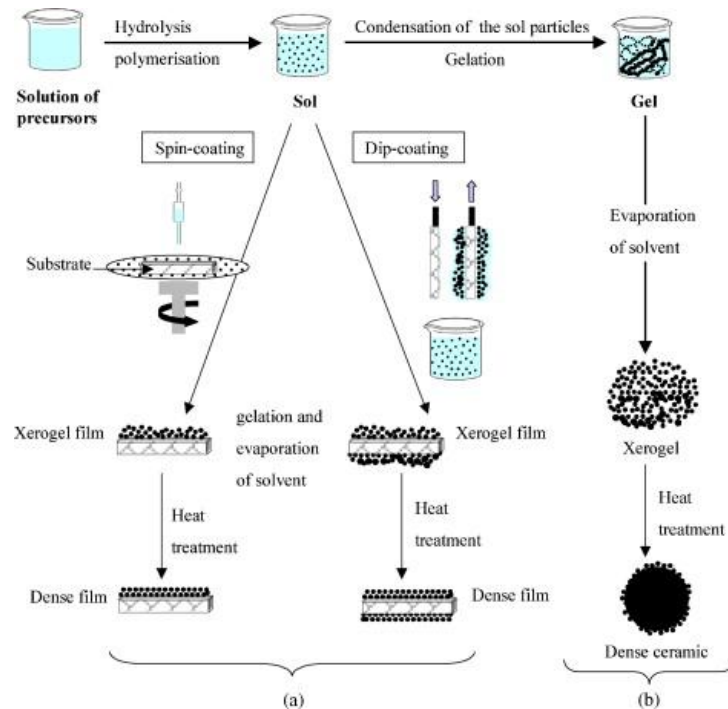


Figure 2. 3. Steps of preparation of (a) thin films and (b) powders by sol gel process.

Source: Reproduced from (Znaidi, L., 2010)

It starts with hydrolysis of the molecular precursor. As reported in the literature review, metal salts in alcoholic solution was used to fabricate ZnO film. Therefore, a solution of inorganic metal salts or metal-organic compound (alkoxide) is used and dissolved in appropriate alcoholic solvent (Levy & Zayat, 2015). Polymerization reaction of precursor forms oxo-, hydroxyl or aqua-bridges (Schodek, Ferreira, & Ashby, 2009; Znaidi, L., 2010). The particles can be extracted by using spin-coated or cast onto a substrate. After that, it undergoes gelation and evaporation of solvent to form a dense or nanoporous film. Solid nanoparticles are obtained through nucleation and growth process. Heat treatment is treated to form a dense film (Pierre, A. C., 1998).

Route two in Figure 2.3 shows the sol undergoes condensation by dehydration. Drying process is required to remove excess solvent. It will cause shrinkage of a gel due to rising of capillary pressure. A dried gel, which is also called as xerogel is formed (Brinker & Scherer, 2013). A dense film is formed by annealing. Sol gel process is used to fabricate thin films, ultrafine particles, nanothickness films and nanoporous membrane.

2.4 Precursor Material

The common salts that are widely used to synthesis ZnO thin films are zinc nitrate hexahydrate, zinc chloride and zinc acetate. Zinc Chloride is used for electrodeposition. The use of high concentration of zinc acetate dehydrate leads to formation of development of thin film morphology. It also leads to formation of ZnO without impurities. With using zinc acetate dehydrate, extra capping agents can be avoided (Akgun, Kalay, & Unalan, 2012).

According to Yahya, (2011), sol gel method was used to fabricate ZnO thin film due to ease of production, low in cost and low temperature needed. In the research, materials that used as precursor of ZnO sol were zinc acetate dehydrate which acted as starting material, monoethanolamine (MEA) and 2-methoxyethanol acted as a stabilizer and as solvent respectively. Anhydrous zinc acetate was used to prevent the induction of large amount of water to the sol gel and to control the reaction. The function of aminoethanols such as monoethanolamine and diethanolamine was to act as ligands to

Zn²⁺ to stabilize the solution against any precipitation, prevent uncontrollable growth of particle, prevent particle from aggregation, and increase the pH due to presence of amine. The ZnO particles were not in perfect spherical shape due to different surface energy of crystallographic directions (Yahya, 2011). Table 2.1 summarizes the sol gel undoped ZnO thin film methods.

Table 2. 1
Sol gel undoped ZnO thin film methods

Authors	Precursor (mol L ⁻¹)	Alcohol	Additive (r)	Aging time	Pre-heat treatment	Post-heat treatment	Ref
Wang et. al.	ZnAc (0.5)	A. EtOH	DEA (1)	-	400	400 - 800	(Wang, et al., 2006)
Natsume and Sakata	ZnAc (0.02)	MeOH	-	-	80	500 - 575	(Natsume & Sakata, 2000)
Liu et. al.	ZnAc (0.6)	EtOH (14 g/L)	DEA (1)	-	100	500	(Liu, Li, Ya, Xin, & Jin, 2008)
Kumar et. al.	ZnAc (0.2)	EtOH	DEA (1)	48 h	250	350 - 450	(Kumar, Kaur, & Mehra, 2007)
Bae and Choi	ZnAc (0.25)	2- PrOH	DEA (1.5)	-	300	400 - 900	(Bae & Choi, 1999)
Zhu et. al.	ZAD (0.75)	2- ME	MEA (1)	-	60	400-550	(Zhu, et al., 2008)
Abdel Aal et. al.	ZAD	2- PrOH	NaOH	-	-	550	(Abdel Aal, Mahmud, & Aboul-Gheit, 2009)
Heridia E. et. al.	ZAD	A. EtOH	MEA	-	200	450	(E. Heridia, et al., 2014)

According to Heridia E., et al., (2014), the ZnO thin films were prepared by sol gel method using precursor solution of zinc acetate dehydrate dissolved in absolute ethanol, deionized water and acetic acid. They revealed that zinc acetate dehydrate had

high solubility in absolute ethanol (E.Heredia, et al., 2014). According to Habibi & Sardashti, (2008), the sol gel process was to control the nano-scale over the structure of a material. By using zinc acetate and MEA as precursor, a stable, transparent and high quality of sol produced (Habibi & Sardashti, 2008).

2.5 Solvent, Absolute Ethanol

Absolute ethanol is been chosen as it gives rise to form spherical shape of particle. This is because absolute ethanol has hydroxyl group to interact with nanoparticle in nucleation, growth and termination process (P.B., Moloto, & Sikhwivhilu, 2012). Hydroxyl group in absolute ethanol also reduces the formation of porosity and irregular grains. Dissolution of ZnAc in absolute ethanol also can lead to self-hydrolysis of zinc salt to form ZnO. Besides that, absolute ethanol forms smaller size of ZnO particles when compared nanoparticles formed when using acetone. The use of alkali is avoided to have better control of purity of final product (Gattorno & Oskam, 2006).

2.6 Thin Film Preparation Method

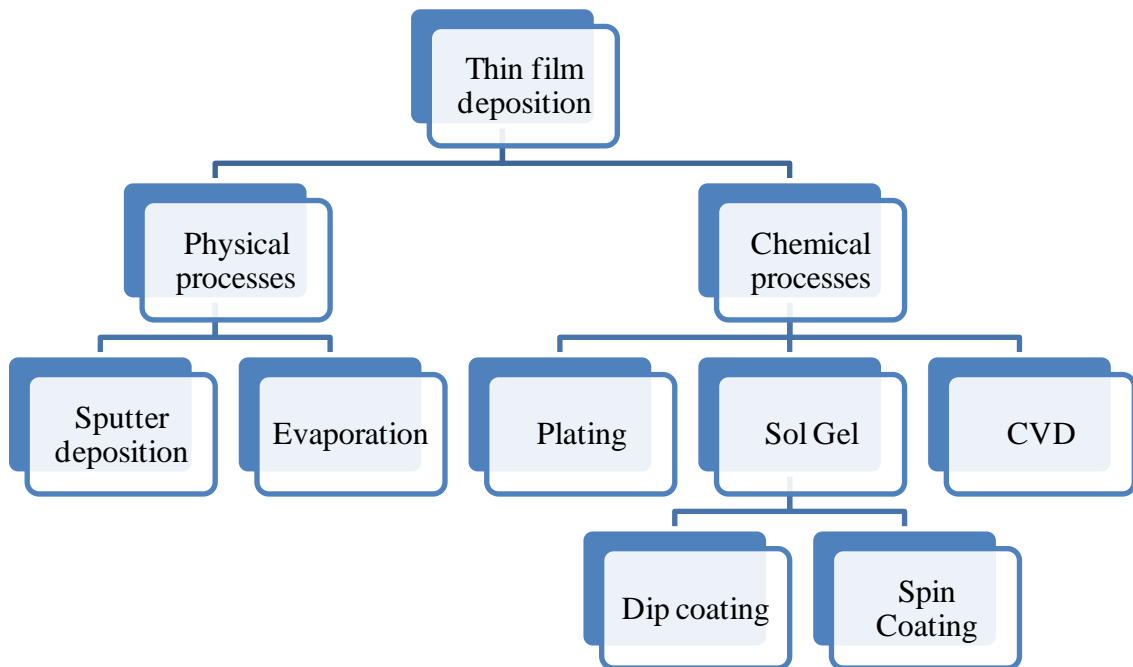


Figure 2. 4. Thin film preparation techniques.

There are many methods in fabricating thin film as shown in Figure 2.4. It divides into chemical deposition (plating, chemical solution deposition, spin coating, chemical vapor deposition, plasma enhanced CVD) and physical deposition (thermal evaporator, sputtering, cathodic arc deposition). In this study, spin coating is used to deposit ZnO thin film on aluminum foil. Spin coating is a simple and fast process for depositing thin coating on a flat substrate. A typical spin coater has a high rotation speeds around 1000-10 000 rpm. The steps of spin coating start with depositing fluid into substrate. Then, accelerating the substrate to final radial velocity. The action of spinning causes the liquid precursor or sol-gel precursor to spread out uniformly on the surface of substrate. The thickness of coating is dependent on the rate of evaporation and the spin speed. Lastly, solvent is evaporated from the film and resulting further thinning film is formed. The typical coating thickness values are below 1 μm (Schweizer & Kistler, 2012).

The advantage of spin coating is that the thickness of film can be easily controlled by changing spin speed or using different viscosity photoresist. Uniform thin film can be formed during coating process. Besides that, spin coating is easy, low cost and fast operating system (Sahu, Parija, & Panigrahi, 2009). It can be used commercially available equipment. It can also be used at all stages of processing on all types of substrate layers. It consumes short time and forms high resist film thickness homogeneity. However, it is highly depending on the position of cavity. Size and shapes of cavities have influence on the resist uniformity. The reproducibility of spin coating is very less.

2.7 Annealing Effect

The process of annealing metal oxide thin film is to control the surface roughness, improve structure and modify surface morphology. The number and size distribution of crystallites depends on annealing temperature and time. Phase transition from amorphous to polycrystallines occurs in annealing process (Monk, Mortimer, & Rosseinsky, 2007).

Shivaraj, et al., (2015) had reported the effect of annealing temperature on the grain size, surface roughness, surface morphology and photoluminescence properties of ZnO thin films prepared by dip coating and spin coating. They were able to observe that when increasing in annealing temperature, the grain size also increased under XRD as shown in Figure 2.5. SEM images showed the surface morphology could be clear distinguished for spin coated film. The study revealed that annealing temperature increased, the wavelength intensity increased under photoluminescence test (Shivaraj, Murthy, Krishna, & Satyanarayana, 2015).

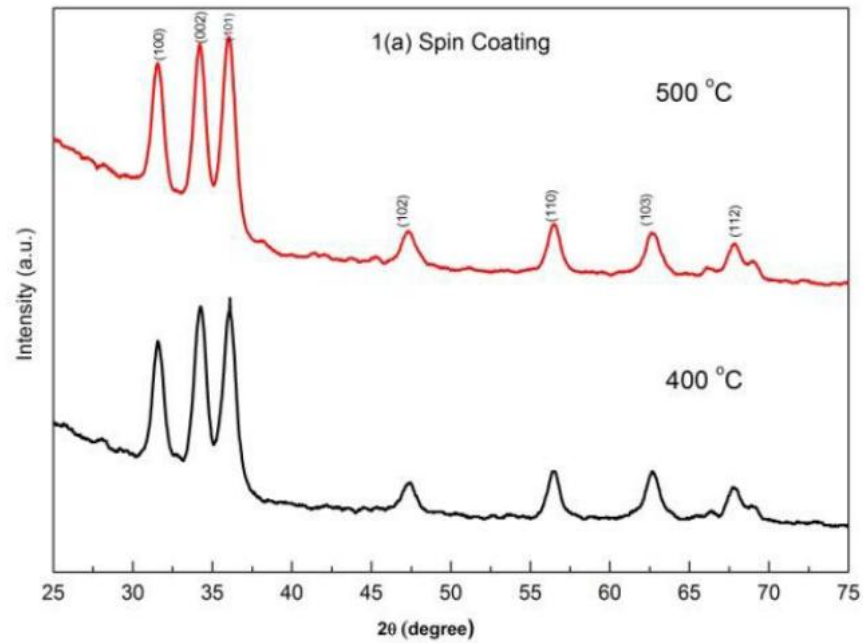


Figure 2.5. XRD pattern ZnO thin film by spin coating at different annealing temperature.

Source: Reproduced from (Shivaraj, Murthy, Krishna, & Satyanarayana, 2015)

2.8 Energy Harvesting Test

Joshi, et al., (2014) revealed that a range of annealing temperature from 100°C to 500°C, the optimum annealing temperature for ZnO thin film was 300°C. ZnO thin film showed highly c-axis oriented, surface morphology with uniformity in grain for this optimum temperature. It presented a better performance with higher peak output volage of 147 mV when testing with vibration sensing performance (Joshi, Nayak, & Rajanna, March 2014).

2.9 Application of Piezoelectric

Piezoelectric transducers generate electricity when a force is applied. They do not need bias voltage. Therefore, piezoelectric materials provide advantages for power harvesting. Piezoelectric transducer connects with two rectifying diode to generate dc

output voltage. The ongoing development of piezoelectric materials has led to huge market. The application of piezoelectric material can be seen from things for daily use to specialized devices, such as air bag sensor, knock sensor, inkjet printers, telephones, ultrasonic imaging and depth sounders.

In 2010, Dr. Ville Kaajakari had developed a microstructured piezoelectric shoe power generator which can be embedded in the sole of a shoe. The design of shoe power generator is shown in Figure 2.6. The transducer could replace the regular heel absorber and generate voltage. The voltage generated could be converted into usable power output to charge battery or powering electronic. He also mentioned that the shoe power generator can be used for powering sensors and locator devices such as Global Positioning System (GPS) which require a milliwatt power source (Ville, K., 2010).



Figure 2. 6. Shoe Power Generator.

Source: Reproduced from (Ville, K., 2010)

Piezoelectric materials are also used in transportation industry. Piezoelectric has been applied in passenger cars, such as knock sensors, distance sensors and fuel injection systems. Distance sensors are used in vehicles as ultrasonic transducer. It is used when parking. When backing, transducer will emit ultrasonic waves. The waves will be reflected back when there is obstacle. The transducer will then received the reflected wave and convert it into electrical system. The distance is calculated from the travelling time of ultrasonic waves (Nuffer & Bein, 2006).

Another application of piezoelectric is self-powered sensors for monitoring of highway bridges. Health monitoring of highway bridges is very important to avoid the loss of human life. Wireless sensor powered by batteries has used to develop health monitoring system for bridges. However, millions of batteries need to be replaced from time to time and high maintenance fees have caused the limitation of wireless sensor. Therefore, energy harvesting is the solution to solve this problem. In 2009, Edward and his team had proposed the testing of wireless sensor system which is powered by energy harvesting on State Route 11 bridge in Potsdam, New York, United State of America. The test showed the feasibility of energy harvesting for the application of Structural Health Monitoring (SHM) (Sazonov, Li, Curry, & Pillay, 2009) . Energy harvesting also can be used in health monitoring of wear detection of train wheels (Wu & Thompson, 2010).

CHAPTER 3

MATERIALS AND METHODS

3.1 Introduction

In this chapter, the research methodology is explained. This research involves four stages which are the procedure of synthesis of ZnO sol gel, fabrication of ZnO film on Al foil as substrate using spin coating technique and heat treatment, characterization of ZnO thin film and piezoelectric test. Spin coating technique was used to fabricate ZnO thin film on Al substrate. ZnO thin film was characterized by using X-ray diffraction (XRD), Field Emission Scanning Electron Microscope (FESEM), Photoluminescence spectroscopy (PL), and Ultraviolet-Visible Spectroscopy (UV-Vis). The piezoelectric test was analysed using vibration as mechanical force.

3.2 Material Synthesis Methods

Figure 3.1 shows the flow chart of research methodology.

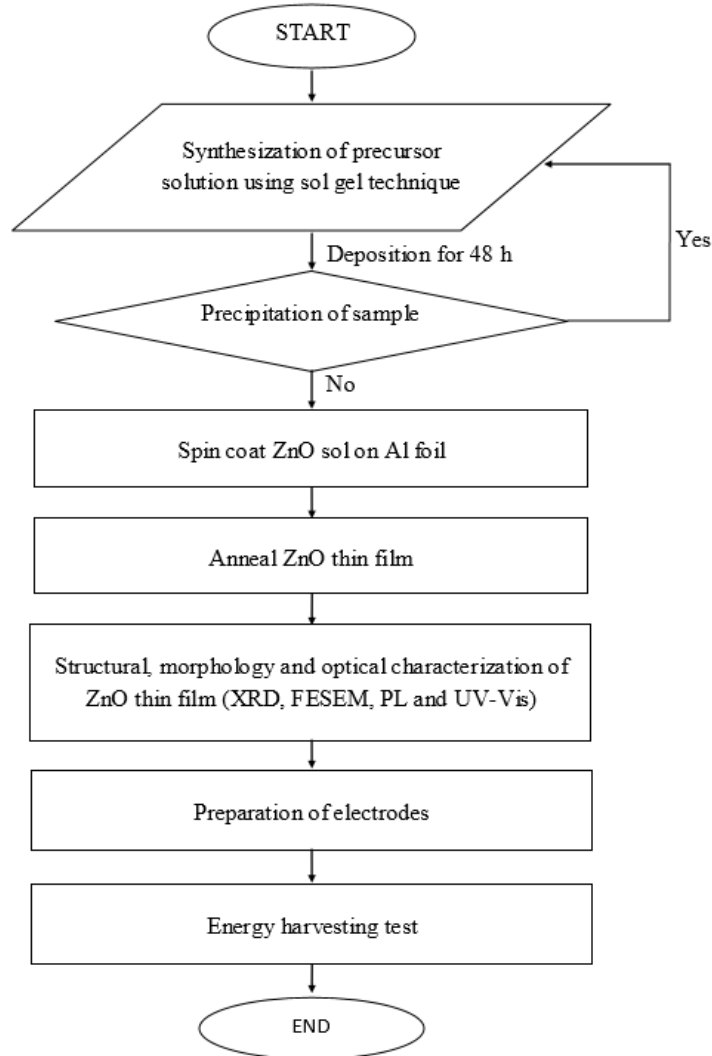


Figure 3.1. Flow chart of methodology research.

3.2.1 Material and Apparatus

The material used in this research were zinc acetate dehydrate (ZnAc), absolute ethanol, ethanol, diethanolamine (DEA). The apparatus used in this research were microscope glass slide, aluminum foil, diamond cutter, magnetic stirrer, hot plate, ultrasonic cleaner, spin coater, carbon tape, and schott bottle.

3.2.2 Preparation of Precursor Solution

Figure 3.2 presents the flow chart of preparation of sol gel by using zinc acetate dehydrate (ZnAc), absolute ethanol and diethanolamine (DEA) as precursor.

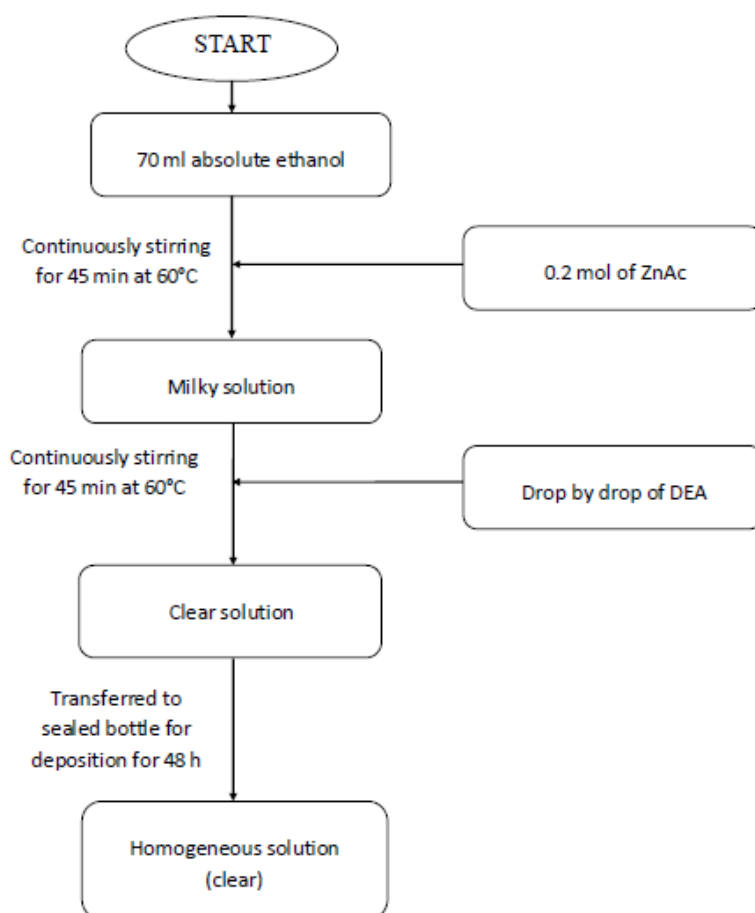


Figure 3.2. Flow chart of preparation of precursor solution.

ZnO sol gel was prepared by dissolving 0.2 mol of zinc acetate dehydrate ($\text{Zn}(\text{CH}_2\text{CO}_2)_2 \cdot 2\text{H}_2\text{O}$) (purity 99.95 %) in 70 ml of absolute ethanol. The mixture was stirred using magnetic stirrer for 45 min at 60 °C. The mixture was become milky as shown in Figure 3.3. Then, diethanolamine (DEA) which acted as stabilizer was added drop by drop to the ZnO sol with interval of 1 min until the solution became clear. The molar ratio of DEA to zinc acetate as 1:1. The addition of DEA was used to affect the change of pH value from neutral to

alkali. The alkaline nature of sol can help the growth of ZnO films. By adding the stabilizer, the sol was become transparent. After another 45 min of stirring, a homogeneous sol was obtained and transferred to a sealed bottle for deposition for 48 h.



Figure 3.3. ZnAc dissolved in absolute ethanol on hot plate.

At the mean time, microscope glass slides were cut with the dimension of 2.5 cm x 2.5 cm. Slides were then washed by ultrasonic cleaner and rinsed with ethanol. Aluminum foil is folded to cover the glass slide. Aluminum foil was also rinsed with ethanol.

3.3 Fabrication Of Zno Thin Film

3.3.1 Spin speed

Laurell WS-650MZ-23 spin coater was used in this research. Figure 3.4 shows spin coating instrument. The ZnO thin film was fabricated on aluminum foil using spin coating technique. In this research, spin speed was acted as one of the manipulated variables.



Figure 3. 2. Spin coating instrument.

A spin coater with 1000-2000 rpm with spinning duration up to 30 s was used. The ZnO sol was spin-coated on the aluminum foil with different speeds (1000 rpm, 1500 rpm and 2000 rpm) for 30 s to fabricate different thickness of ZnO thin film. After deposition, the films were preheated at 60 °C for 30 s using a hot plate. The spinning process and preheating process were repeated for 5 times to get 5 layers. Finally, the samples were transferred to high temperature furnace and annealed at 300 °C for 1 h to ensure the complete oxidation, eliminate the organic residue and promote the complete crystallization of ZnO thin films. Figure 3.5 shows the ZnO film formed with spin speed of 2000 rpm and annealing temperature of 300 °C.

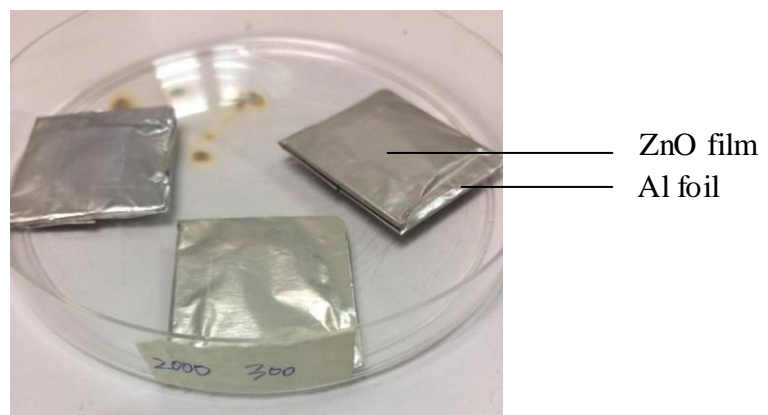


Figure 3.3. ZnO film formed with spin speed of 2000 rpm and annealing temperature of 300 °C.

3.3.2 Heat Treatment

ZnO sol was spin-coated on the aluminum foil at a speed of about 1500 rpm for 30 s. After deposition, the films were preheated at 60 °C for 30 s using a hot plate. The spinning process and preheating process were repeated for 5 times to get 5 layers. After that, the samples were annealed at different temperatures (300 °C, 400 °C and 500 °C) for 1 h using a high temperature vacuum furnace.

3.4 Characterization of ZnO Thin Film

The ZnO films were characterized by X-ray diffraction (XRD), Field Emission Scanning Electroscopy Microscope (FESEM), Photoluminescence spectroscopy (PL) and Ultraviolet-visible spectroscopy (UV-Vis) as shown in Figure 3.6. The compositions of ZnO thin films were observed under XRD technique. The morphologies of films were investigated using FESEM with an acceleration of 15 kV and beam current of 20 mA. The optical properties of films were analysed using PL and UV-VIS spectroscopy.

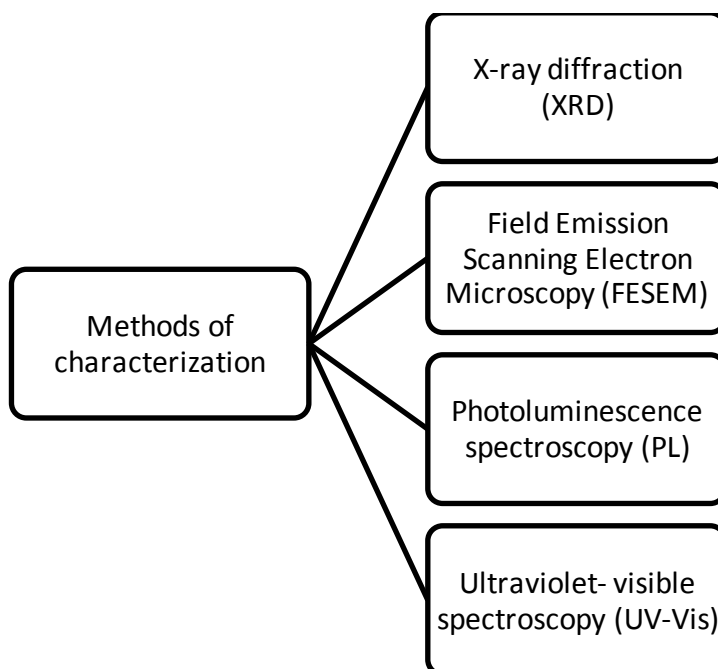


Figure 3.4. List of methods used to characterize the ZnO films.

3.4.1 X-ray Diffraction (XRD)

X ray diffraction is a non-destructive technique. The ZnO films were analyzed using X-ray diffraction (XRD) to examine the composition, crystalline size and phase exists. The instrument used was Miniflex II, Rigaku, Japan. The ZnO films were scanned in $2\theta = 10-80^\circ$ at the rate of $0.1^\circ/\text{min}$ with $\text{Cu K}\alpha$ ($\lambda = 1.5406 \text{ \AA}$) radiation. The films with 5 layers were too thin and could not be detected. Therefore, 35 layers of ZnO film was formed for XRD detection.

3.4.2 Field Emission Scanning Electron Microscopy (FESEM)

Zeiss EVO 50 Scanning Electron Microscope and Baltec-SCD 005 Sputter Coater were used to characterize surface morphology and thickness of ZnO films as shown in Figure 3.7.



Figure 3. 5. FESEM instrument (a) Zeiss EVO 50 SEM and (b) Baltec-SCD 005 Sputter Coater

The area of ZnO films was cut using scissor. The ZnO films with aluminum foil were mounted on aluminum stub and attached using sticky carbon tape. A layer of platinum was coated on the top of sample holder using sputtering. The purpose of coating platinum as conductive layer was to avoid electron charging and image degradation. The surface morphology and grain size

of ZnO films were analysed using FESEM. For each sample, few areas were detected randomly with different magnification.

For measuring the thickness of the film, ZnO sol was coated on glass which act as substrate. The ZnO films with glass substrates were cut with diamond cutter. Then, the glass substrates with films were mounted on aluminum stub with vertical position and attached using sticky carbon tape. A layer of platinum was coated on the top of sample holder by sputtering. The thickness of ZnO films were analysed. For each sample, few areas were detected randomly with different magnification.

3.4.3 UV-VIS Spectroscopy

Shimadzu UV-1800 spectrophotometer and UVProbe 2.43 software were used to analyse the optical properties of ZnO film. Two microscope glass slides were rinsed with ethanol. Then, they were placed in S compartment and R compartment respectively to set the baseline. The wavelength was set from 200 nm to 1400 nm. A chime sound was played and the glass slides in S compartment was taken out and replaced with glass slide that coated with ZnO film. The first peak was observed at long wavelength region. It was marked and the value of wavelength was observed and used in calculation.

3.4.4 Photoluminescence Spectroscopy

FLS 920 Fluorescence Spectrometer and F900 software were used to analyse the photoluminescence property of ZnO film. Glass slide coated with ZnO thin film was placed in sample compartment. A glass slide with 330 nm was placed in the spectrometer to act as filter. The value of estimated excitation wavelength was filled and the EML wavelength was filled as 400 nm. The range of emission scan was filled from 320 nm to 640 nm. A bell-shaped graph was observed and the peak of the photoluminescence was marked.

3.5 Piezoelectric Test

Piezoelectric test was carried out to measure the voltage that can be produced by the piezoelectric material, ZnO. Branson CPX 5800 H Ultrasonic bath and multimeter were used to measure the voltage.

Carbon tape which acted as a conductive electrode was connected with ZnO film. Copper wire was connected with two different electrodes, which are aluminum foil and carbon tape and multimeter to complete the circuit. Figure 3.8 showed the connection of copper wire with two electrodes. The sample was placed on the surface of the water. The schematic diagram for piezoelectric testing is shown in Figure 3.9. Ultrasonic cleaner was then switched on. 40 kHz of frequency was applied to the water within three minutes. The readings for maximum voltage and minimum voltage are video recorded.



Figure 3. 6. Connection of copper wire with two electrodes.

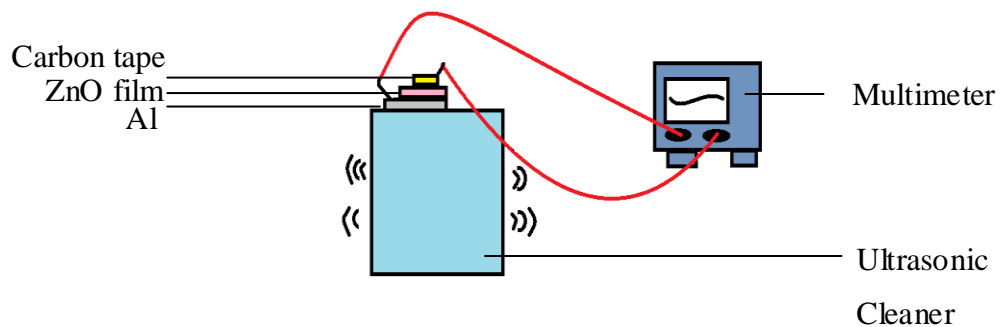


Figure 3. 7. Schematic diagram of piezoelectric testing.

CHAPTER 4

RESULTS AND DISCUSSION

4.1 Introduction

This chapter consists of the results of the characterization of sample and piezoelectric test. The XRD results showed the diffraction phase of each film. All the films showed preferentially oriented at $\sim 65^\circ$ which corresponding to (1 1 2) diffraction phase. From FESEM results, surface morphology of ZnO films showed all the films were successfully formed as nano size grains. However, there were some agglomeration and cracks could be found on the surface. ZnO films were not homogeneous completely. From the result of UV-Vis, ZnO films were excited at 340 ~ 363 nm. They were excited at ultraviolet region. The band gap of all the films were around 3.4 ~ 3.6 eV which are higher than theoretical band gap value (3.37 eV). The annealing temperature was increased, the energy band gap was decreased. From results of photoluminescence, ZnO thin film were emitted electron at 380 ~ 390 nm. Ultrasonic vibration test was used to determine the voltage that can be produced by ZnO films. The sample that could produce the highest voltage was ZnO film with spin speed of 2000 rpm and annealing temperature of 300 °C. The maximum voltage produced was 27.3 mV and minimum voltage was 0.4 mV. The sample that produced the least voltage was ZnO film with spin speed of 1500 rpm and annealing temperature of 400 °C with average voltage of 1.368 mV.

4.2 Synthesis and Characterization of ZnO Thin Film

4.2.1 X-Ray Diffraction Analysis

The crystalline size, phase orientation and lattice parameter of ZnO film were calculated from XRD result. From XRD result, the crystalline size of crystal can be calculated using Scherrer's formula which is shown in Eq. (4.1).

$$T = \frac{0.9 \lambda}{\beta \cos \theta} \quad (4.1)$$

where T is the crystallite size in nano meter, λ is wavelength of x-ray (1.5406 Å), β is full width at half maximum of the peak (FWHM) in radian and θ is the Bragg's angle.

The Bragg's law was used in this research to calculate the crystal structure, therefore d-spacing of the crystal can be calculated from Eq. (4.2).

$$n\lambda = 2d \sin \theta \quad (4.2)$$

where λ is the wavelength, n is number of order, d is lattice spacing, and θ is the diffraction angle.

The lattice parameter of hexagonal crystal structure can be calculated from the Eq. (4.3).

$$\frac{1}{d^2} = \left(\frac{4}{3}\right) \frac{h^2 + kh + k^2}{a^2} + \frac{l^2}{c^2} \quad (4.3)$$

where value of d is the lattice spacing which obtained from equation 4.2, h, k and l are the Miller indices of each peak, a and c are the lattice parameters.

The films were grown by sol-gel technique on Al foil as substrate with different spin speed and annealing temperature. All films that formed were polycrystalline. In Figure 4.1, the film grown with spin speed speed of 1000 rpm and annealing temperature of 300 °C presented two peaks at 43.99° and 64.447° which corresponding to the (1 0 1) and (1 1 2) diffraction planes of hexagonal ZnO. The d-spacing of the crystal was 1.44570 Å whereas the lattice parameter calculated was $a = 0.352$ nm and $c = 0.507$ nm.

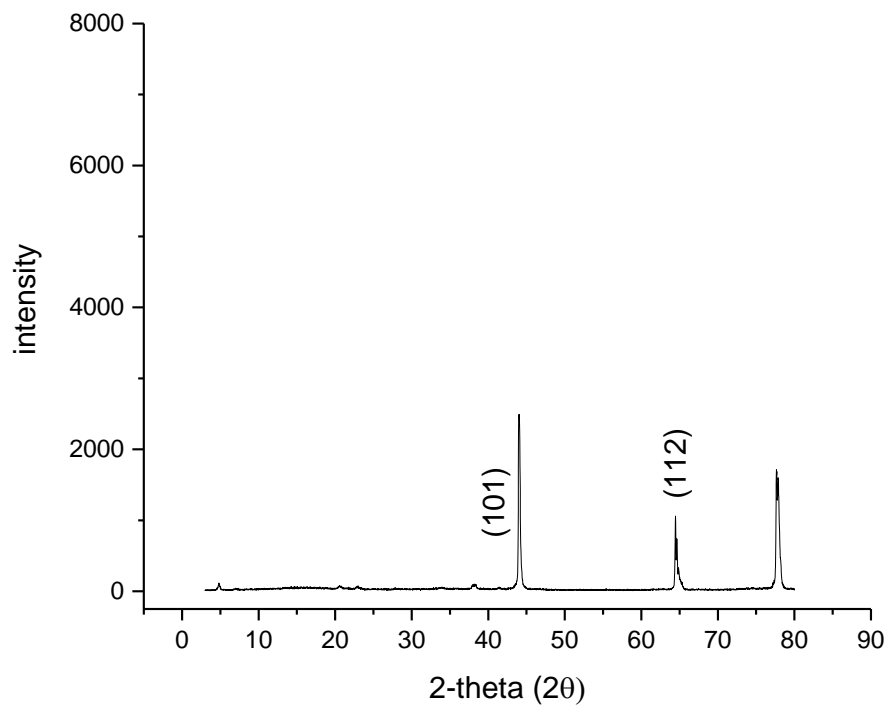


Figure 4. 1. XRD pattern of ZnO thin film with spin speed of 1000 rpm and annealing temperature 300 °C.

In Figure 4.2, the film grown with spin speed of 1500 rpm and annealing temperature of 300 °C presented two peaks at 65.1421° and 74.04°. These peaks correspond to the (1 1 2) and (0 0 4) diffraction phases of ZnO wurtzite structure. The d-spacing of the crystal was 1.4308 Å and the lattice parameter was calculated as $a = 0.345$ nm and $c = 0.5116$ nm.

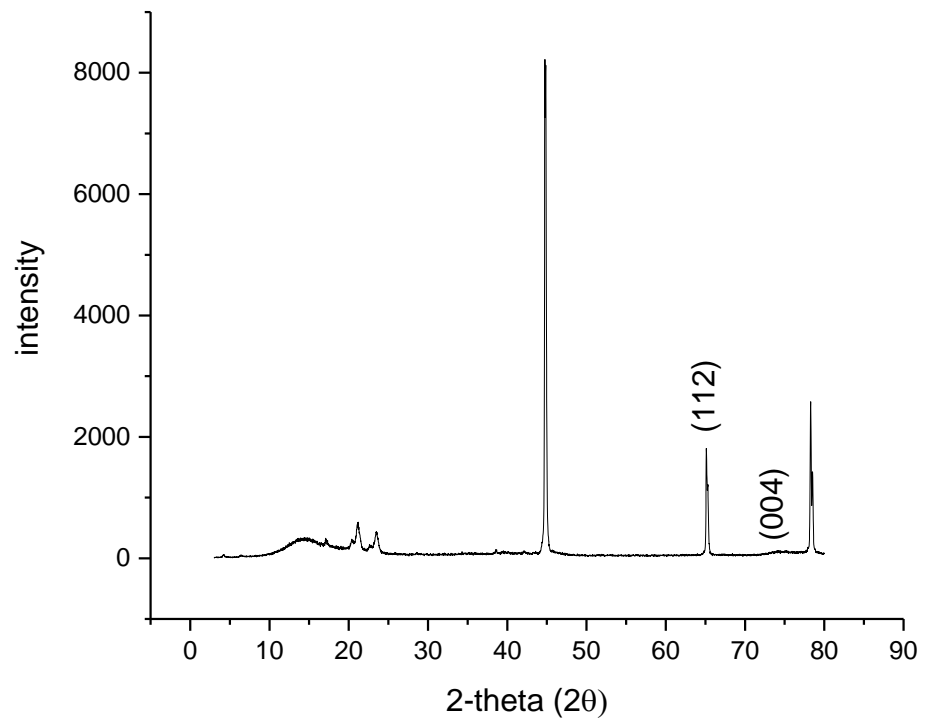


Figure 4. 2. XRD pattern of ZnO thin film with spin speed of 1500 rpm and annealing temperature 300 °C.

In the pattern of film with spin speed of 2000 rpm and annealing temperature of 300 °C as shown in Figure 4.3, three peaks could be clearly seen at 34.37°, 65.083° and 78.394°. These peaks were corresponding to (0 0 2), (1 1 2) and (1 0 4) diffraction planes of ZnO wurtzite structure respectively. The d-spacing used was 1.43199 Å and the lattice parameter for ZnO film was calculated as $a=0.3427$ nm and $c=0.5214$ in plane (1 1 2).

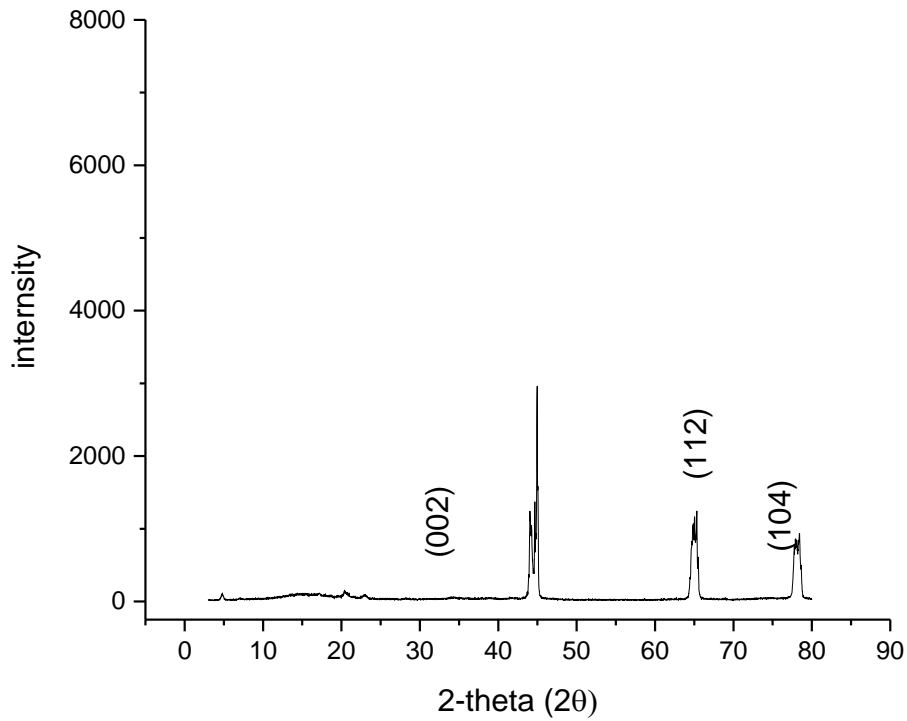


Figure 4. 3. XRD pattern of ZnO thin film with spin speed of 2000 rpm and annealing temperature 300 °C.

The diffraction phase of (0 0 2) could be also found at the film with spin speed of 1500 rpm and annealing temperature of 400 °C and 500 °C at 34.47° and 33.61° respectively. The (0 0 4) of diffraction phase also could be found at the peak of 74.1° of film with annealed at 400 °C as shown in Figure 4.4. The d-spacing used for film with annealed at 400 °C was 1.43303 Å and lattice parameter was $a = 0.3435$ nm and $c = 0.52$ nm in plane (1 1 2) at 65.03 °.

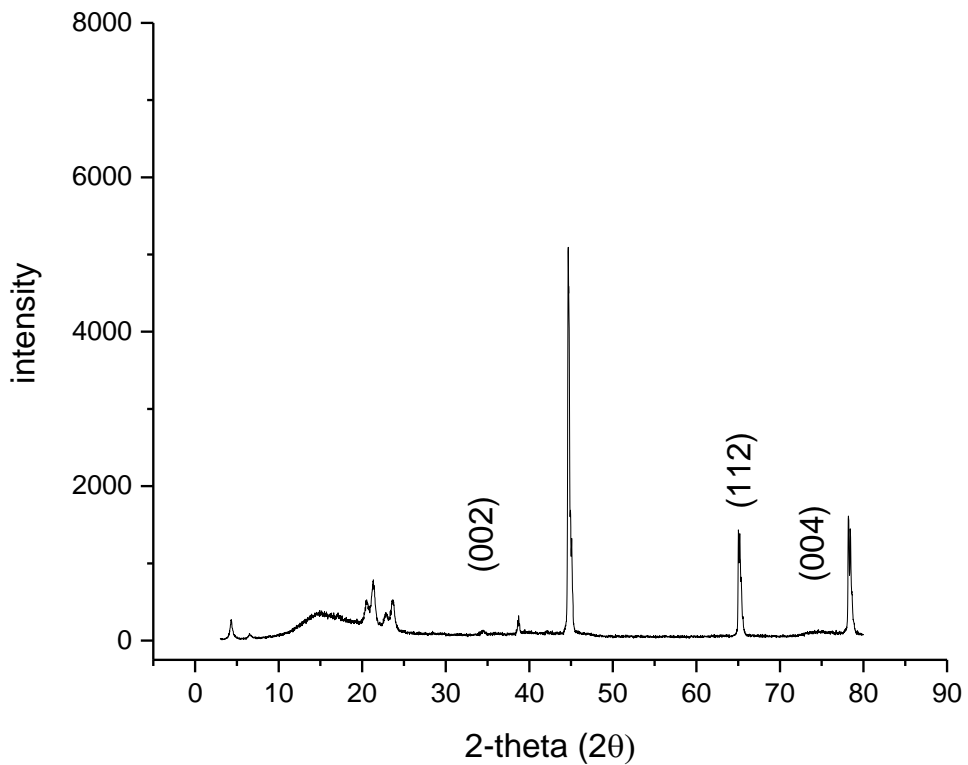


Figure 4. 4. XRD pattern of ZnO thin film with spin speed of 1500 rpm and annealing temperature 400 °C.

Figure 4.5 shows film with spin speed of 1500 rpm and annealing temperature of 500 °C could also find diffraction phase of (1 1 2) and (2 0 2) at the peaks of 64.882° and 75.5°. The d-spacing of this film was 1.43594 Å and lattice parameter was $a= 0.341$ nm and $c= 0.5328$ nm.

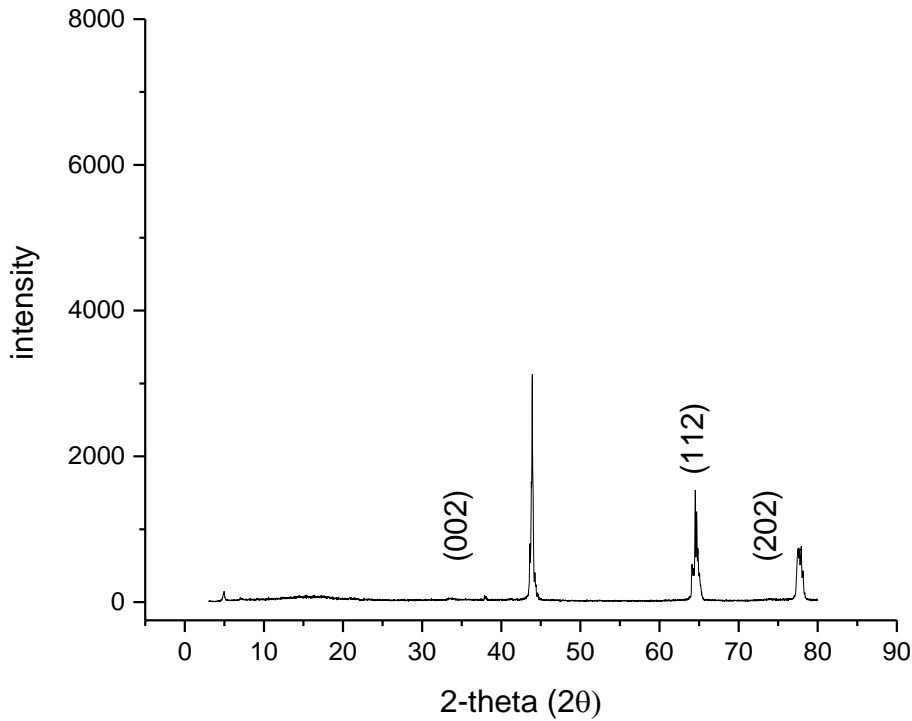


Figure 4. 5. XRD pattern of ZnO thin film with spin speed of 1500 rpm and annealing temperature 500 °C

From Figure 4.1 to 4.5, the highest peak was $\sim 45^\circ$. The peak was corresponding to aluminum plane as shown in Appendice A1 (Manikandan, Gopal, & Chun, 2016). For the plane of ZnO, it could be found that all the films were preferentially oriented in the (1 1 2) direction at $\sim 65^\circ$. The typical phase (0 0 2) was only found at some films. The presence of (0 0 2) diffraction phase was due to the precursor solution used was ZnAc which promotes the growth of crystal in (0 0 2) direction (Sagar, et al., 2007). Some of the films could not find the peak of (0 0 2) may due to destructive interference happened. Figure 4.6 showed the combination of XRD spectrum of ZnO films. When the annealing

temperature was increased, the intensity peak was decreased. This was due to the large thermal expansion coefficient between ZnO film and substrate.

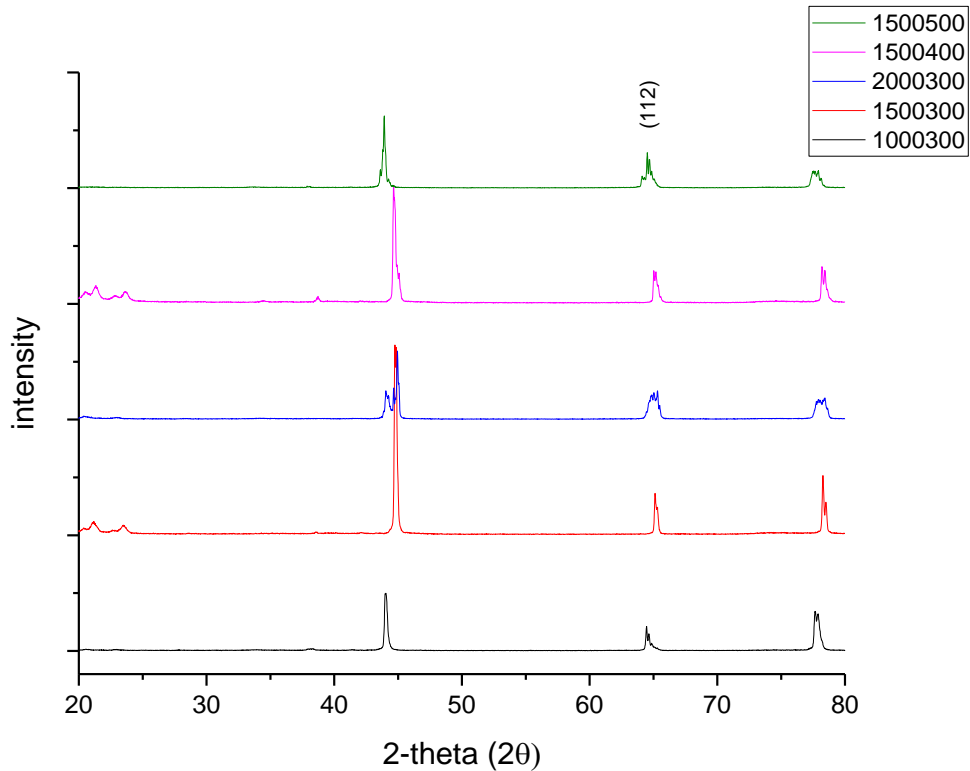


Figure 4. 6. XRD spectrum of each film.

Table 4.1 shows the average crystallite size of ZnO films with different spin speed and annealing temperature. When the annealing temperature was increased, the crystallite size was increased. The crystallite size was decreased from 0.5832 nm to 0.4955 nm and to 0.4512 nm. It had shown that temperature could affect material crystal sizes.

Figure 4.7 shows the ZnO film with rotation speed of 1500 rpm and annealing temperature of 180 °C. The ZnO film formed by dissolving 0.5 mol of ZnAc into 20ml of absolute ethanol. The mixture was stirred until the solvent evaporated and white powder formed. Then, DEA was added in and a clear gel was formed. The peaks of XRD spectrum were at 33.06 ° and 64.669 ° which corresponding to (1 1 1) and (1 1 2) diffraction plane.

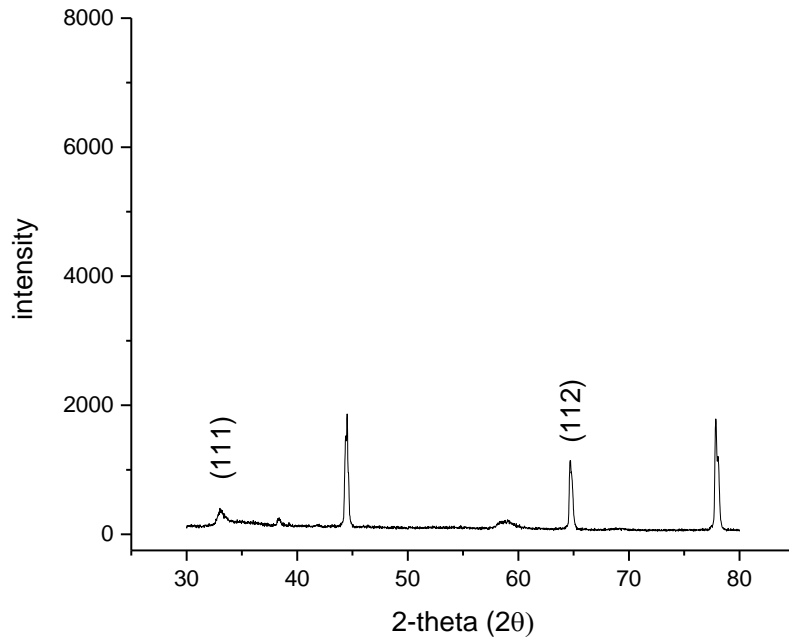


Figure 4. 7. XRD spectrum of ZnO film with spin speed of

1500 rpm and annealing temperature of 180 °C.

Table 4. 1

(h k l) plane, d-spacing and crystalline size for the ZnO thin films with different spin speed and annealing temperature

Sample	Spin Speed (rpm)	Anneal Temperature (°C)	2θ (°)	(h k l)	d-spacing	FWHM	Average Crystalline Size, nm
A	1000	300	43.9918	(1 0 1)	2.0566	0.181	0.8405
			64.4470	(1 1 2)	1.44570	0.174	
B	1500	300	65.1421	(1 1 2)	1.43083	0.151	0.5832
			74.0400	(0 0 4)	1.27900	2.260	
C	2000	300	34.3700	(0 0 2)	2.60700	1.100	0.4878
			65.0830	(1 1 2)	1.43199	0.260	
			78.3940	(1 0 4)	1.21882	0.256	
D	1500	400	34.4700	(0 0 2)	2.60000	0.560	0.4955
			65.0300	(1 1 2)	1.43303	0.142	
			74.1000	(0 0 4)	1.27800	2.500	
E	1500	500	33.6100	(0 0 2)	2.66400	0.900	0.4512
			64.8820	(1 1 2)	1.43594	0.143	
			75.5000	(2 0 2)	1.25900	4.000	

4.2.2 Morphology Analysis

The morphology of ZnO films were characterized under FESEM. The morphology of ZnO films could not be studied under SEM due to limitation of magnification of SEM spectroscopy.

shows the nanoparticle size with different condition and annealing temperature. The grain size was increased when the annealing temperature was increased. This is because the fusion of grains was happened due to increment of energy (Quinones-Galvan, et al., 2013). Figure 4.8 until Figure 4.12 show the surface morphology of films with different magnification.

Table 4. 2
Nanoparticle size of ZnO films with different spin speed and annealing temperature

Sample	Spin speed (rpm)	Annealing temperature (°C)	Grain size (nm)
A	1000	300	19.00
B	1500	300	17.98
C	2000	300	20.38
D	1500	400	20.63
E	1500	500	25.15

By using FESEM, cross section of ZnO film was also been analysed. ZnO film was coated on glass substrate to examine the thickness. ZnO film that was coated on Al substrate could not be examined as when cutting, ZnO film was bent and overlap with Al foil. Therefore, by using Al foil as substrate, ZnO layer and Al layer could not be differentiated. Figure 4.13 shows the failure of examining cross section of ZnO film on Al substrate. The method used in Figure 4.13 was backscattered mode. Figure 4.14 to Figure 4.18 show the cross section of ZnO film on glass substrate with different magnification at several parts of sample.

It was observed that the thickness was decreased due to increasing of spin speed. Comparing between Figure 4.9, Figure 4.11 and Figure 4.12, the thickness was increased when annealing temperature was increased. It was due to the grain size was increased when annealing temperature was increased. Therefore, the thickness was increased. Table 4.3 shows the average thickness of ZnO film with different spin speed and annealing temperature.

Figure 4.8 shows the surface morphology of ZnO film with spin speed of 1000 rpm and annealed at 300 °C with different magnification at several regions of the sample. The surface of ZnO film did not form uniformly. Some parts of sample had agglomerated. Figure 4.8 (b), (c) and (d) were taken at the part of uniform surface. It could be seen that the grains formed were as small as nano size. The grain size was around 15 – 20.6 nm.

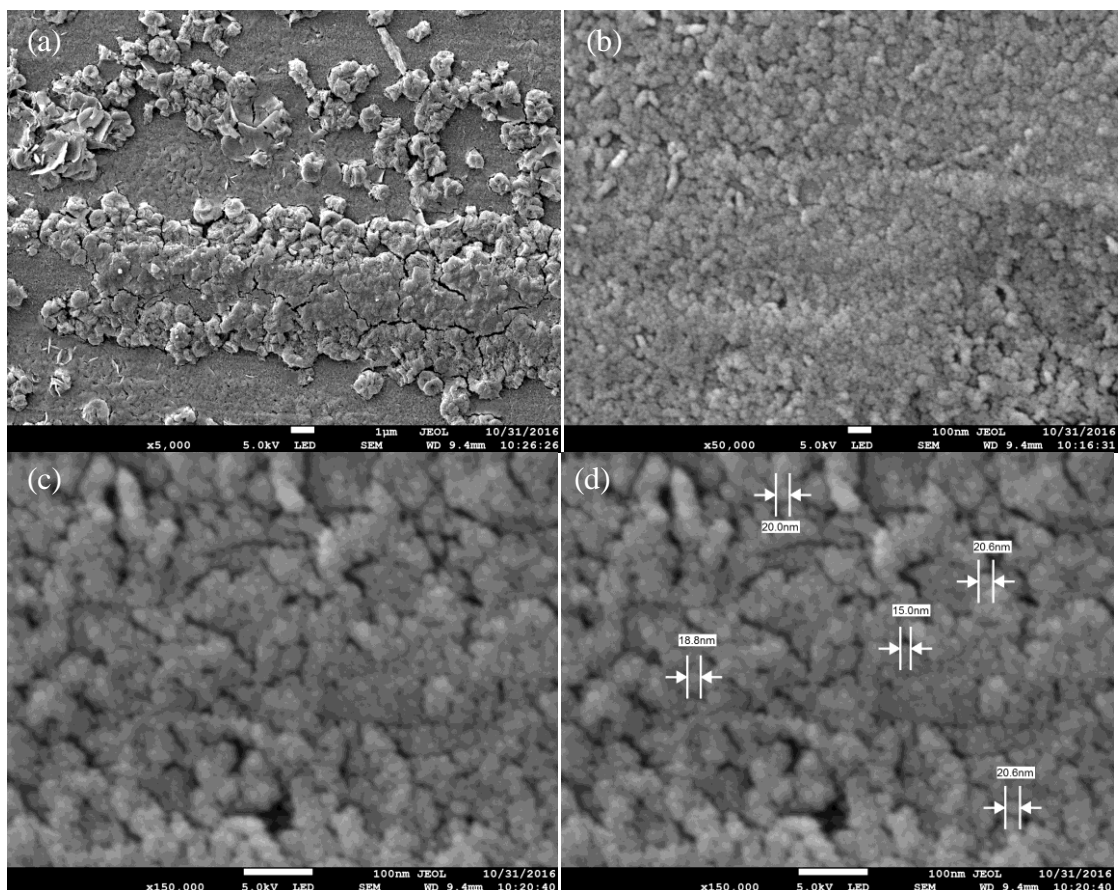


Figure 4.8. Surface morphology of ZnO thin with spin speed of 1000 rpm and annealed at 300 °C with different magnification (a) 5 kx, (b) 50 kx, (c) 150 kx (d) 150 kx with measurement.

Figure 4.9 shows the surface morphology of ZnO thin with spin speed of 1500 rpm and annealed at 300 °C with different magnification at several regions of the sample. It could be seen that the film was uniformly formed but with cracking. Figure 4.9 (b), (c) and (d) were taken at the part of uniform surface without cracking. The grain size of ZnO was around 16.9 – 20 nm.

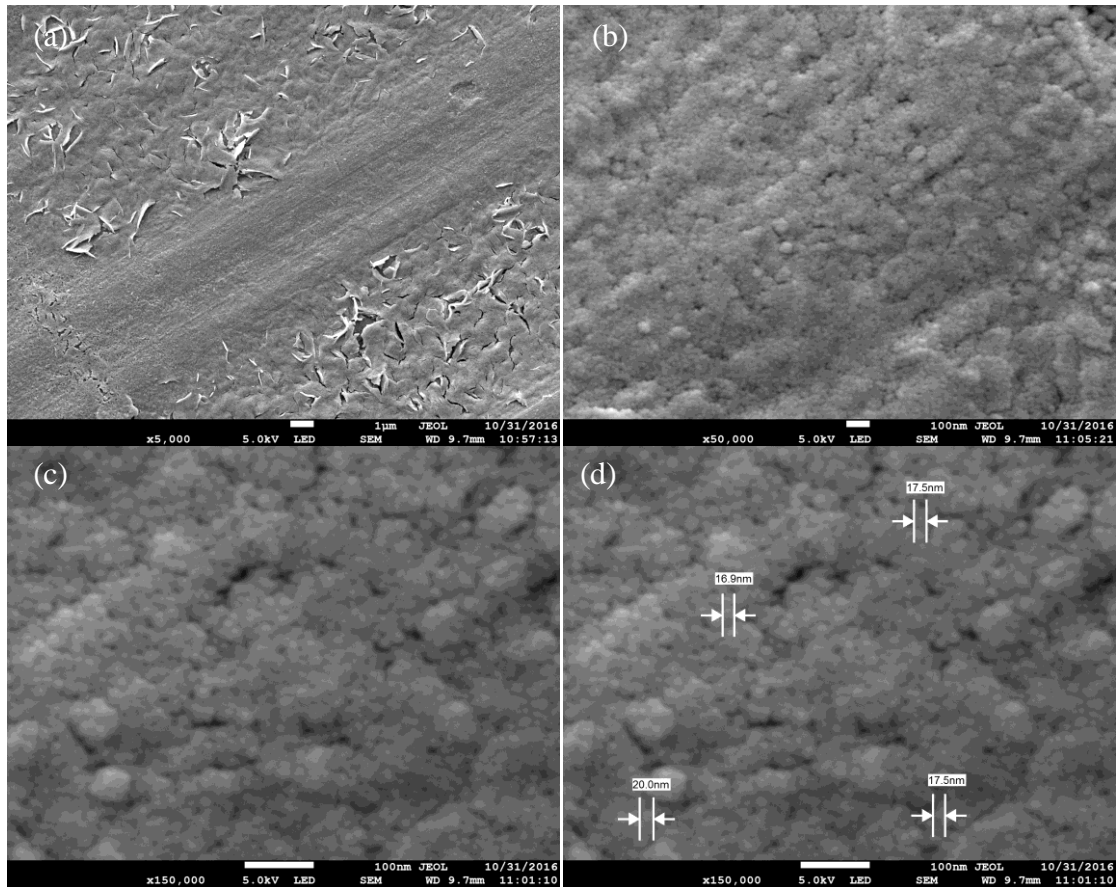


Figure 4.9. Surface morphology of ZnO thin with spin speed of 1500 rpm and annealed at 300 °C with different magnification (a) 5 kx, (b) 50 kx, (c) 150 kx (d) 150 kx with measurement.

Figure 4.10 shows the the surface morphology of ZnO thin with spin speed of 2000 rpm and annealed at 300 °C with different magnification at several regions of the sample. It could be seen that the film was uniformly formed but with porosity. Figure 4.10 (b), (c) and (d) were taken at the part of uniform surface without porosity. The grain size of ZnO was around 18.8 – 21.9 nm.

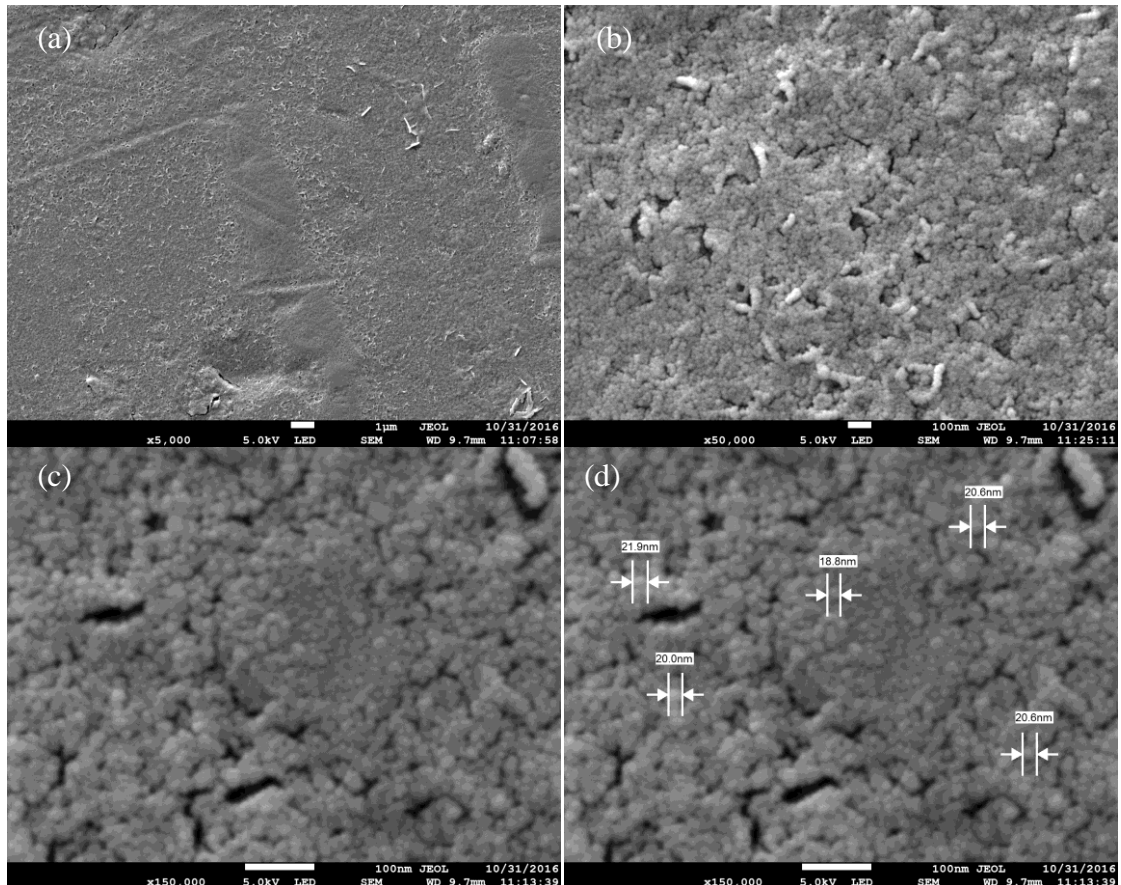


Figure 4.10. Surface morphology of ZnO thin with spin speed of 2000 rpm and annealed at 300 °C with different magnification (a) 5 kx, (b) 50 kx, (c) 150 kx (d) 150 kx with measurement.

Figure 4.11 shows the surface morphology of ZnO thin with spin speed of 1500 rpm and annealed at 400 °C with different magnification at several regions of the sample. It could be seen that the film was uniformly formed but with cracking. Figure 4.11 (b), (c) and (d) were taken at the part of uniform surface without any defect. The grain size of ZnO was around 20 – 21.9 nm. When comparing with figure 4.9, the grain size of ZnO was increased due to annealing temperature was increased.

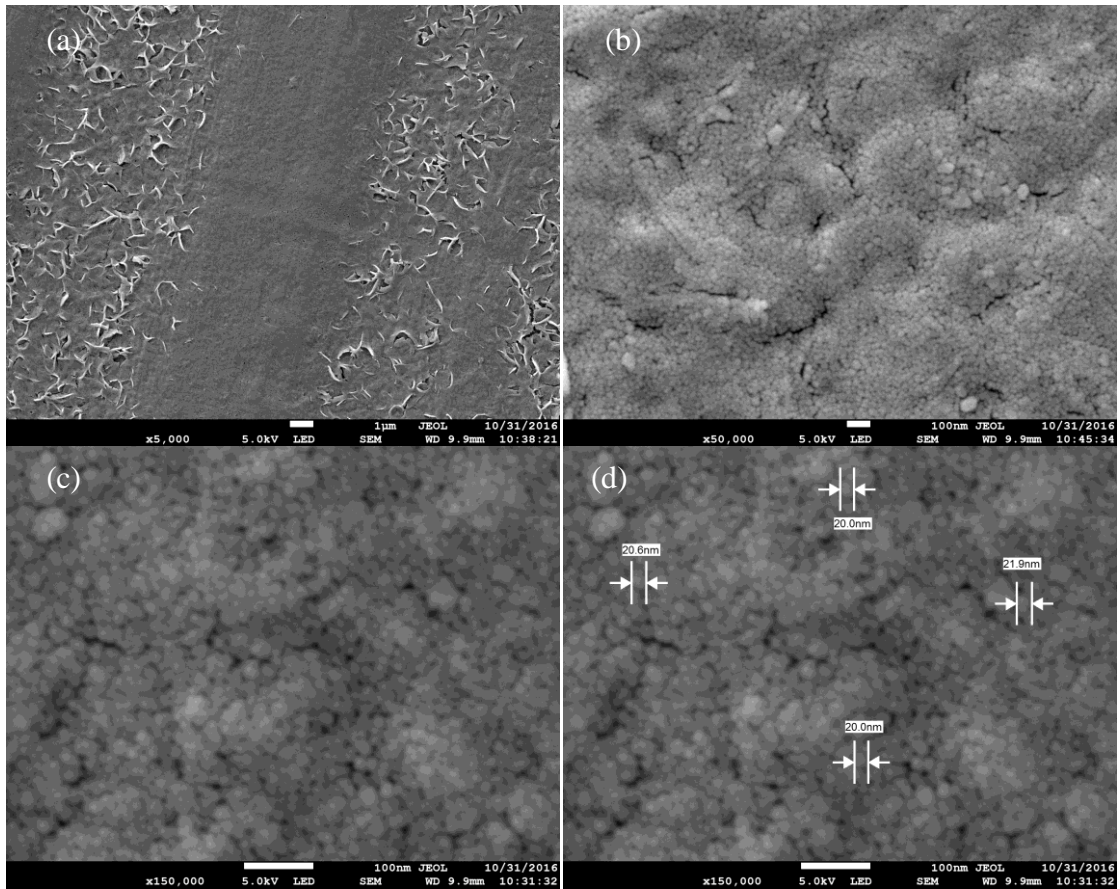


Figure 4.11. Surface morphology of ZnO thin with spin speed of 1500 rpm and annealed at 400 °C with different magnification (a) 5 kx, (b) 50 kx, (c) 150 kx (d) 150 kx with measurement.

Figure 4.12 shows the surface morphology of ZnO thin with spin speed of 1500 rpm and annealed at 500 °C with different magnification at several regions of the sample. It could be seen that the film was uniformly formed but with cracking and porosity. Figure 4.12 (b), (c) and (d) were taken at the part of uniform surface without any defect. The grain size of ZnO was around 23.7-26.9 nm. When comparing with figure 4.9 and figure 4.11, the grain size of ZnO was increased due to annealing temperature was increased.

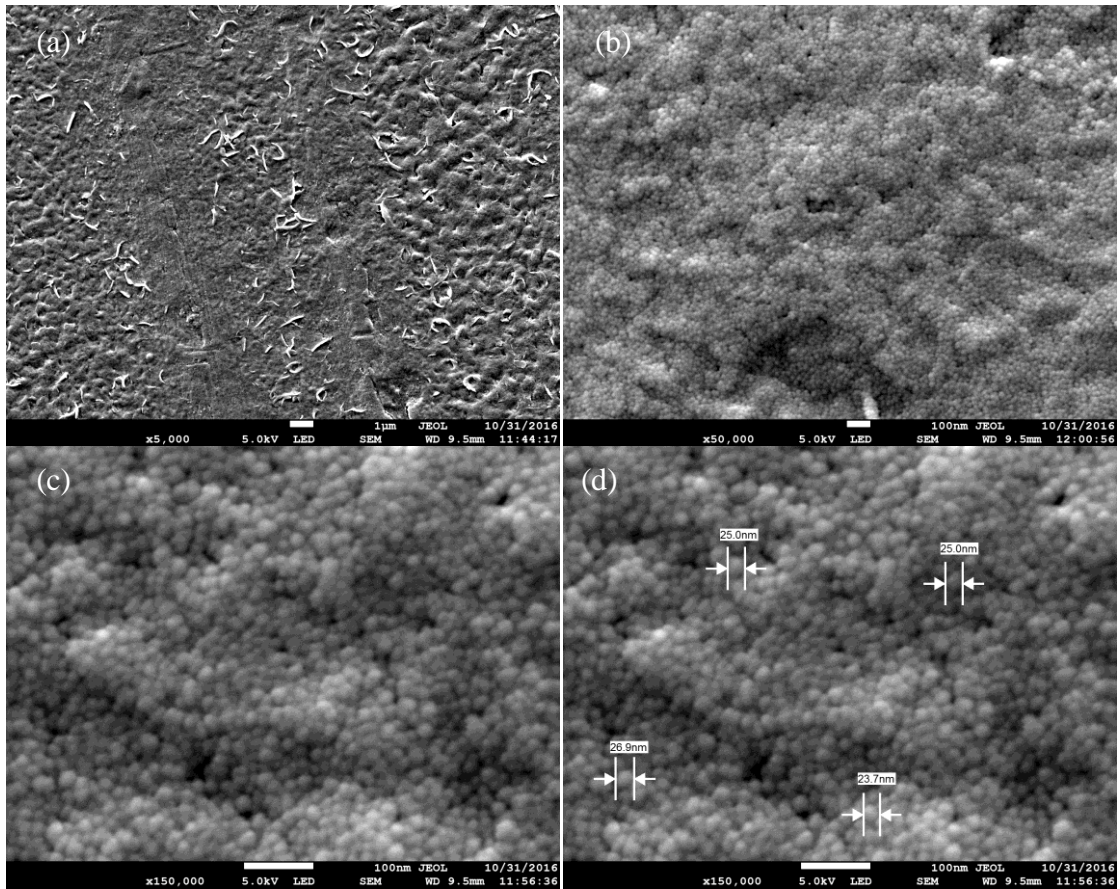


Figure 4.12. Surface morphology of ZnO thin with spin speed of 1500 rpm and annealed at 500 °C with different magnification (a) 5 kx, (b) 50 kx, (c) 150 kx (d) 150 kx with measurement.

Figure 4.13 shows the cross section of ZnO film on Al substrate with spin speed of 1000 rpm and annealed at 300 °C. Figure 4.13 (a) was used the backscattered mode. The purpose was to detect the changes in chemical contrast. Therefore, ZnO film and Al substrate can be differentiated. In theoretically, ZnO would have denser color than Al foil as the molecular weight and atomic number was higher than Al. However, from figure 4.12 (a), there was no difference in color. Therefore, the cross section of ZnO film on Al substrate could not be determined. The method had changed to ZnO coated on glass substrate. This was due to glass substrate is brittle. ZnO film would not bend or overlap onto glass substrate. Diamond cutter was used to cut glass substrate in order to get thickness.

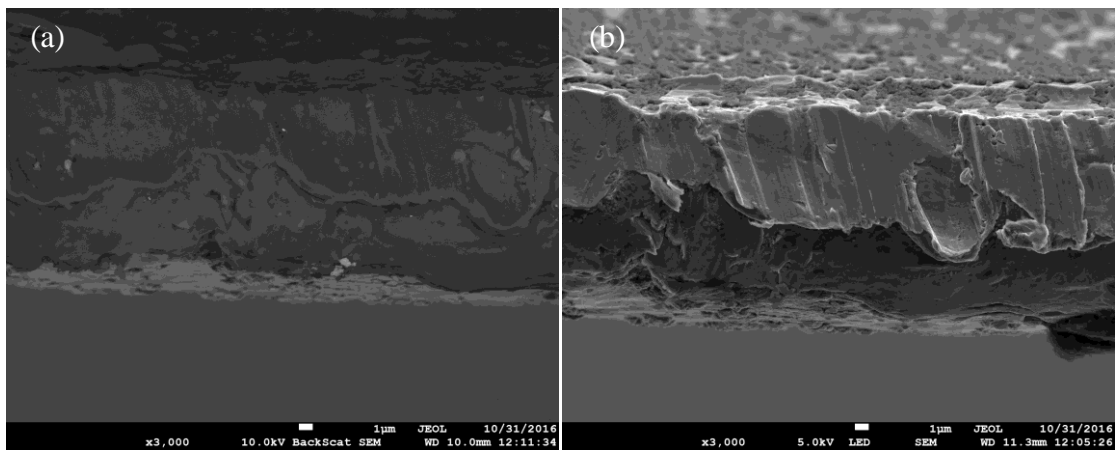


Figure 4.13. Cross section of ZnO film on Al substrate with spin speed of 1000 rpm and annealed at 300 °C.

Figure 4.14 shows the cross section of ZnO film with spin speed of 1000 rpm and annealed at 300 °C with different magnification at several parts of sample. From the cross section, it could be found that some parts of ZnO film was not uniformly formed. From figure 4.14 (d), it could be seen that there were some ZnO particle overlapped with glass substrate. This might due to the improper cutting process. The thickness of ZnO film was 373 nm.

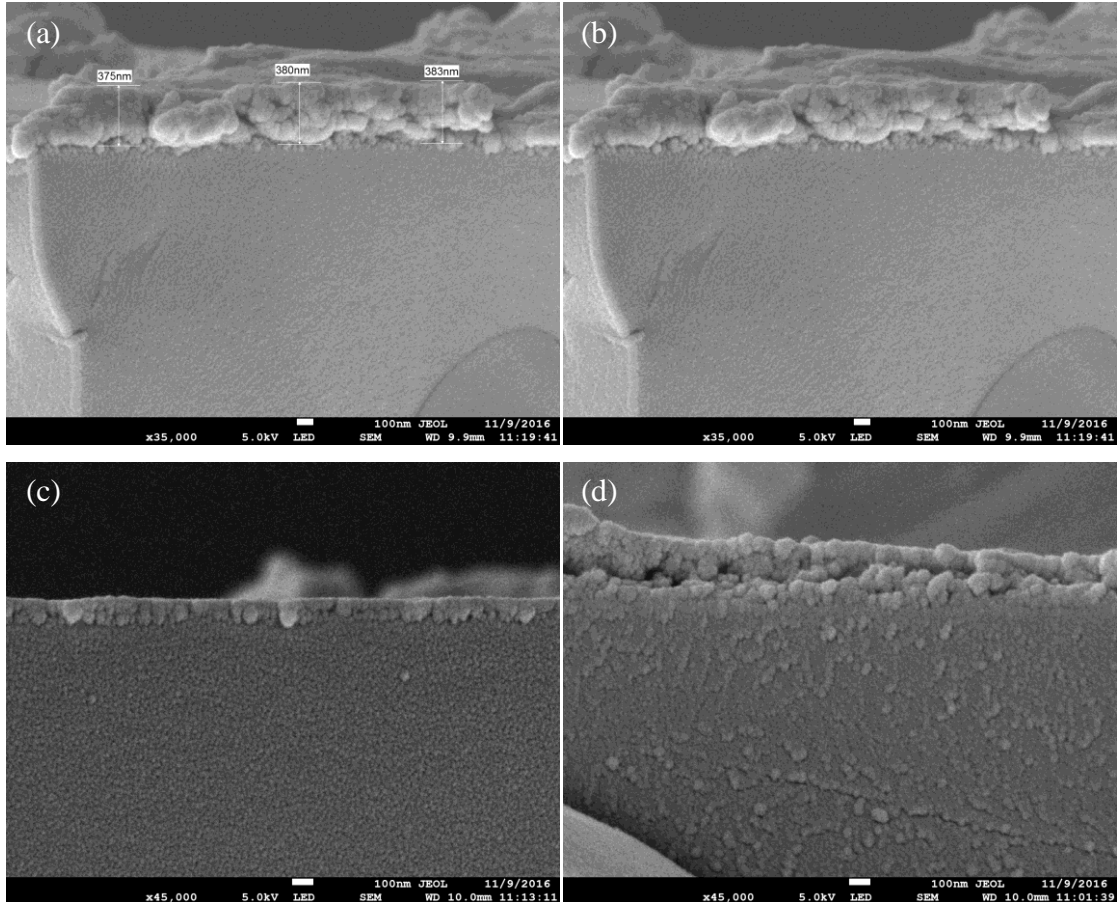


Figure 4.14. Cross section of ZnO film with spin speed of 1000 rpm and annealed at 300 °C with different magnification at several parts of sample.

Figure 4.15 shows cross section of ZnO film with spin speed of 1500 rpm and annealed at 300 °C with different magnification at several parts of sample. From the cross section, it could be found that ZnO film was uniformly formed. The thickness of ZnO film was 166.25 nm.

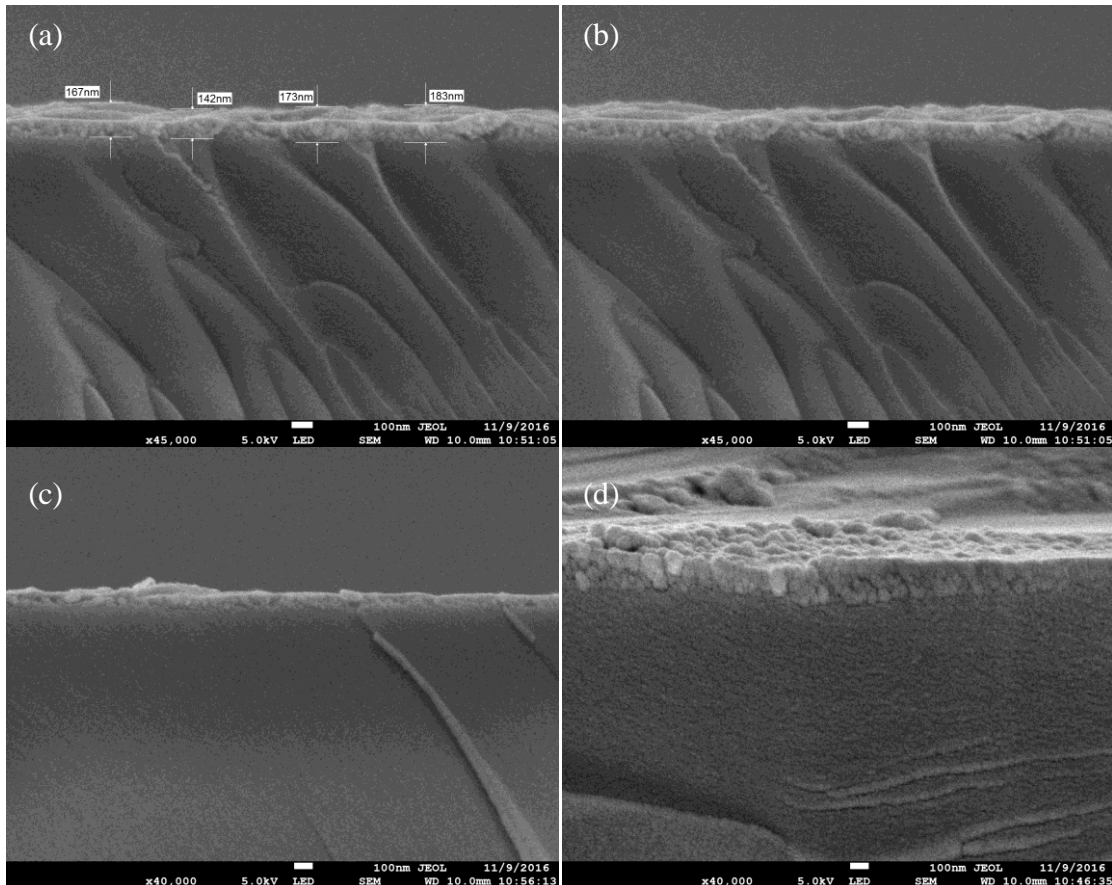


Figure 4. 15. Cross section of ZnO film with spin speed of 1500 rpm and annealed at 300 °C with different magnification at several parts of sample.

Figure 4.16 shows the cross section of ZnO film with spin speed of 2000 rpm and annealed at 300 °C with different magnification at several parts of sample. From the cross section, it could be found that ZnO film was uniformly formed. The thickness of ZnO film was 113.25 nm.

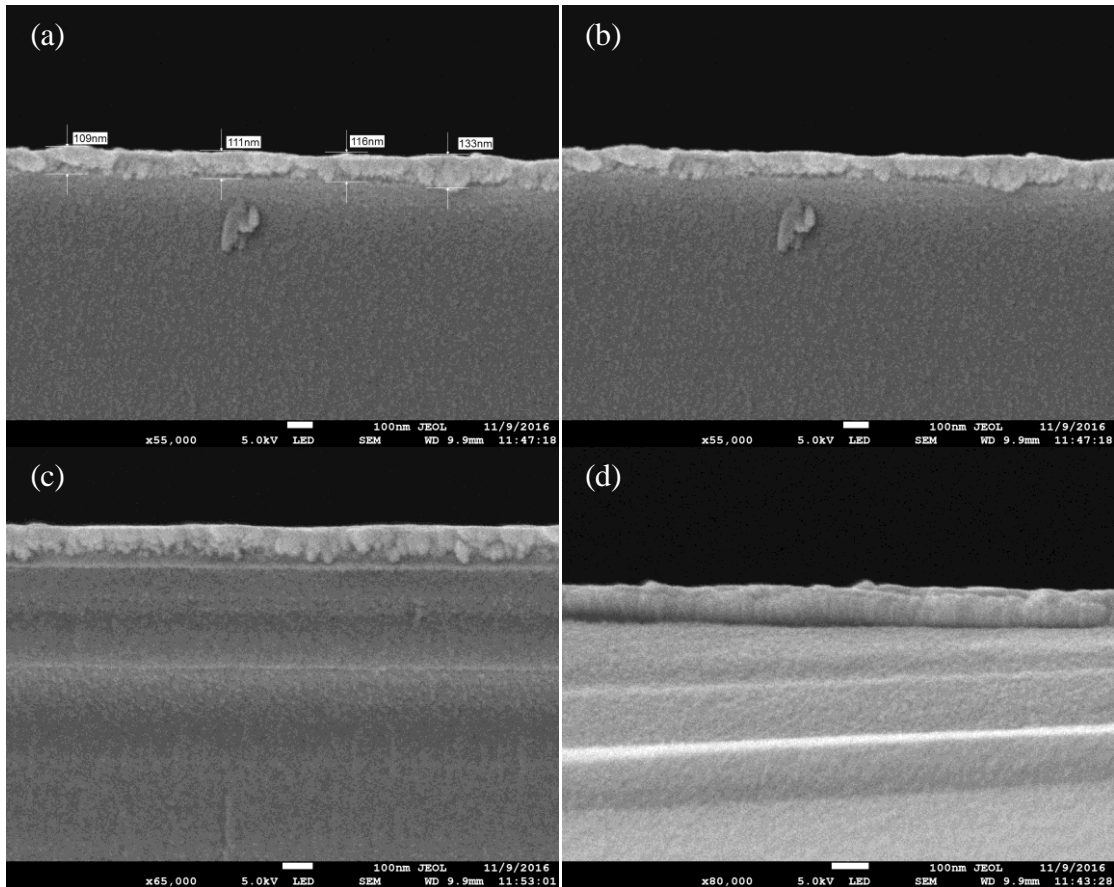


Figure 4.16. Cross section of ZnO film with spin speed of 2000 rpm and annealed at 300 °C with different magnification at several parts of sample.

Figure 4.17 shows the cross section of ZnO film with spin speed of 1500 rpm and annealed at 400 °C with different magnification at several parts of sample. From the cross section, it could be found that some parts of ZnO film was not uniformly formed. The thickness of ZnO film was 187.5 nm.

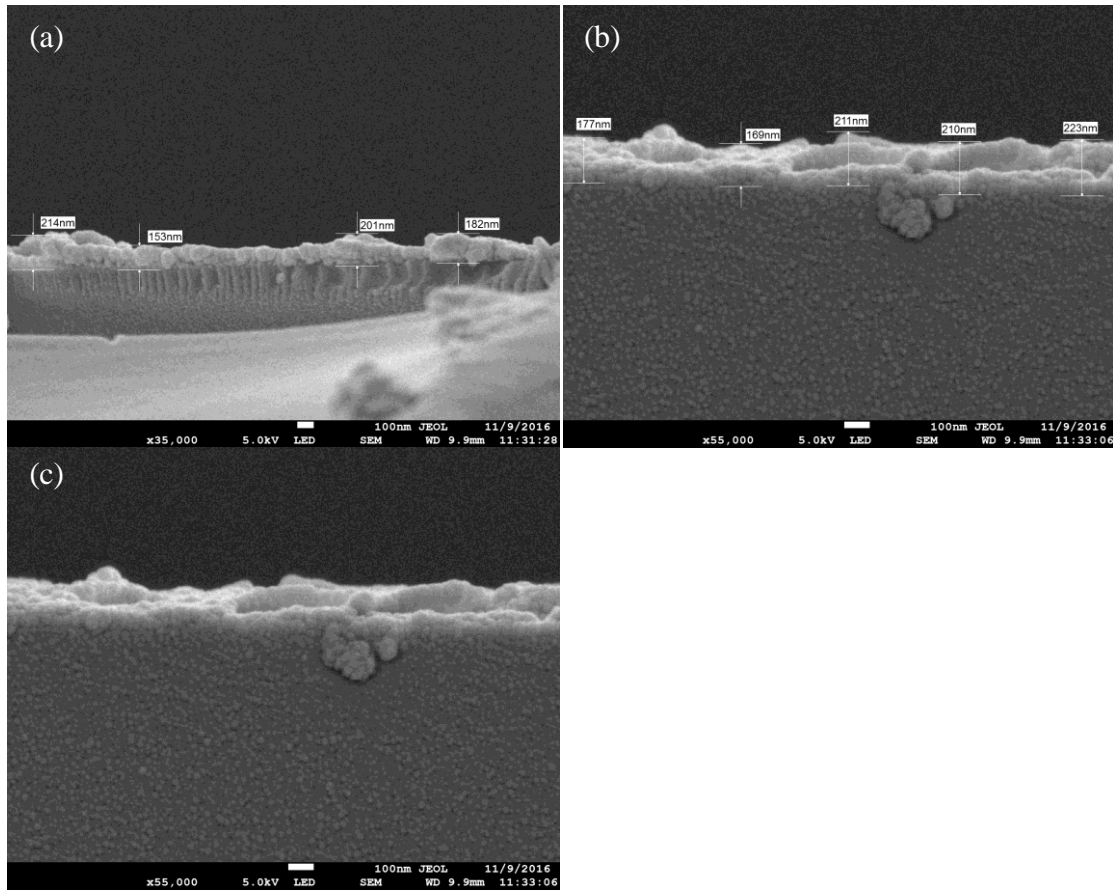


Figure 4.17. Cross section of ZnO film with spin speed of 1500 rpm and annealed at 400 °C with different magnification at several parts of sample.

Figure 4.18 shows the cross section of ZnO film with spin speed of 1500 rpm and annealed at 500 °C with different magnification at several parts of sample. From the cross section, it could be found that some parts of ZnO film was uniformly formed. The thickness of ZnO film was 205.25 nm.

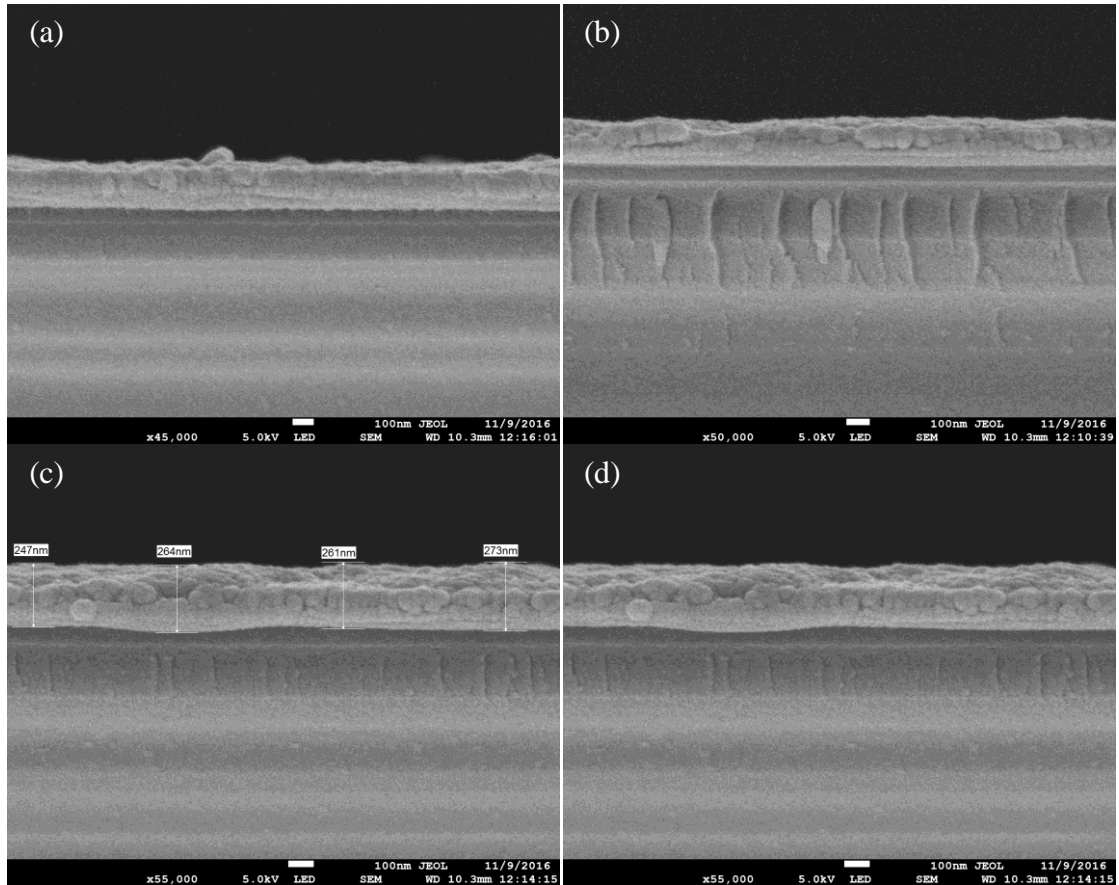


Figure 4.18. Cross section of ZnO film with spin speed of 1500 rpm and annealed at 500 °C with different magnification at several parts of sample.

Figure 4.19 shows the surface morphology of ZnO film with spin speed of 1500 rpm and annealing temperature of 180 °C. It could clearly observed that the nanoparticle did not form in this film. This was because the film did not have enough energy to form nanoparticle.

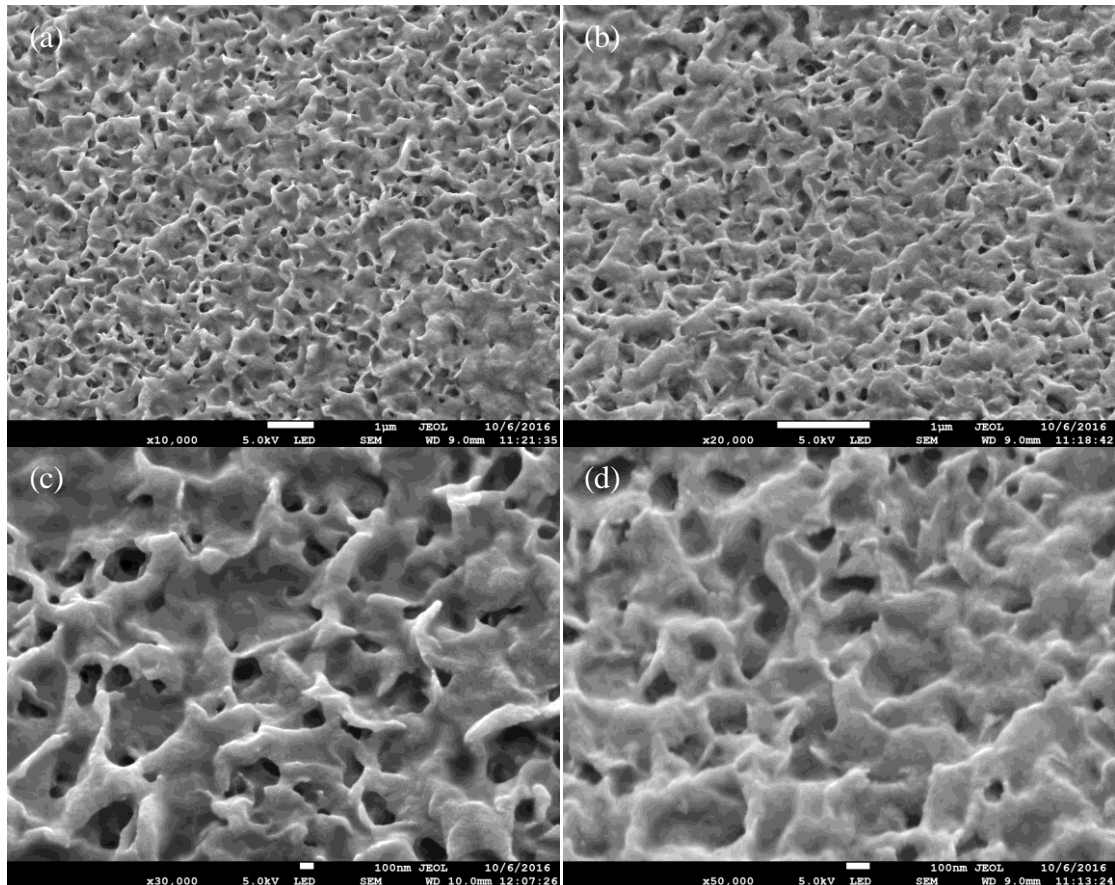


Figure 4.19. Surface morphology of ZnO film with spin speed of 1500 rpm and annealing temperature of 180 °C.

Table 4. 3

Thickness of ZnO thin film with different spin speed and annealing temperature

Sample	Spin Speed (rpm)	Annealing Temperature (°C)	Average Thickness (nm)
A	1000	300	373.00
B	1500	300	166.25
C	2000	300	113.25
D	1500	400	187.50
E	1500	500	205.25

4.2.3 Photoluminescence

PL spectra of ZnO films were shown in Figure 4.20. The emission spectrum of ZnO thin film showed the peak was at narrow band ~380 nm. It was corresponding to band edge emission. It was due to free exciton emission. It has ultraviolet region. The PL spectrum also showed a wide broad peak of green emission at ~500 nm. The green emission was due to the existence of intrinsic defects, which are zinc vacancies and oxygen interstitial (Xu, Zheng, Lai, & Pei, 2014) . It could be observed that when the annealing temperature was increased, the wavelength intensity was increased. This was because of the oxygen and zinc atoms in interstitial site moved to lattice sites. It was also due to surface grain area increases (Li, Xu, Li, Shen, & Wang, 2010). From Figure 4.20, it can be seen that there was insignificant change in wavelength, this is because the wavelength shift only caused by composition of precursor but not annealing temperature and spin speed. Annealing temperature had only changed the intensity of wavelength (Sagar, et al., 2007).

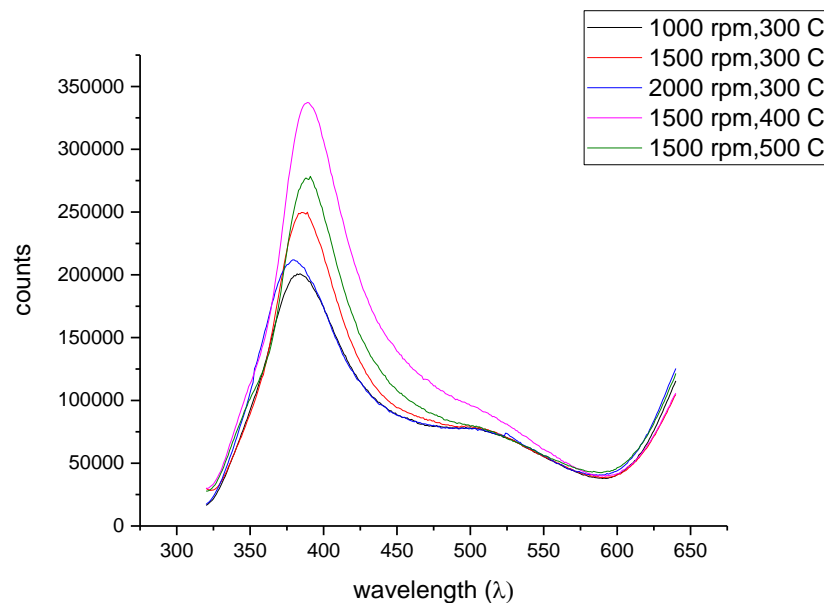


Figure 4. 20. PL spectrum of ZnO thin film with different spin speed and annealing temperature.

4.2.4 UV-Vis Analysis

UV-Vis was carried out to calculate the band gap of ZnO nanoparticles. The first excitonic peak was determined by Origin Pro software. The first excitonic peak was corresponding to the electron transition from valence band to conductive band. The band gap of ZnO film could be calculated using Eq. (4.4).

$$E_g = \frac{hv}{\lambda} \quad (4.4)$$

where E_g is energy band gap of ZnO, h is Plank's constant in eV (4.135×10^{-15}), v is the velocity of light (3×10^8) and λ is the wavelength of first excitonic peak.

From Figure 4.21 to Figure 4.25 show the UV emission spectrum of ZnO with different spin speed and annealing temperature. Table 4.4 showed the energy band gap of each ZnO film with different spin speed and annealing temperature. It could be found that when increasing the annealing temperature, the energy band gap was decreased. The highest band gap (3.6109 eV) was belong to ZnO film with spin speed of 1000 rpm and annealing temperature of 300 °C.

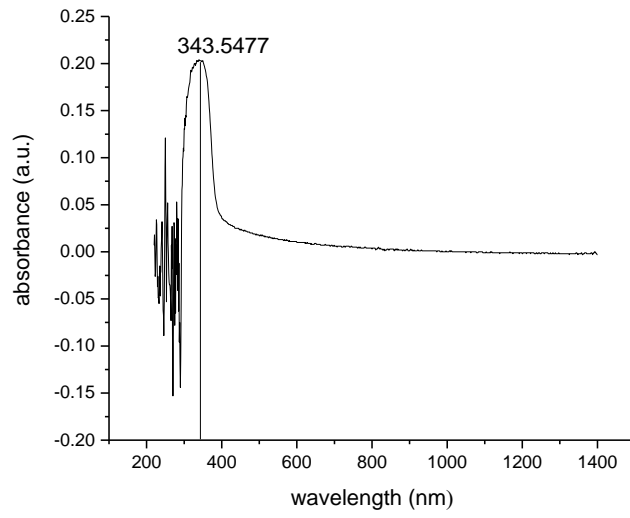


Figure 4. 21. UV spectrum of ZnO film with spin speed of 1000 rpm and annealing temperature of 300 °C.

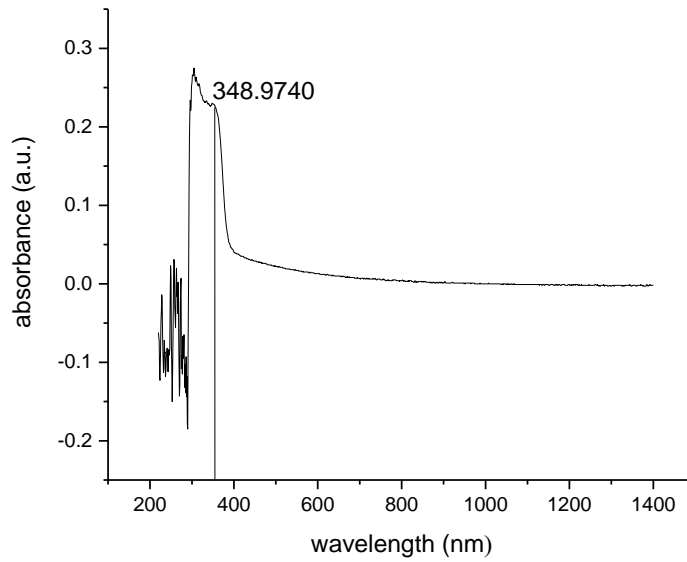


Figure 4. 22. UV spectrum of ZnO film with spin speed of 1500 rpm and annealing temperature of 300 °C.

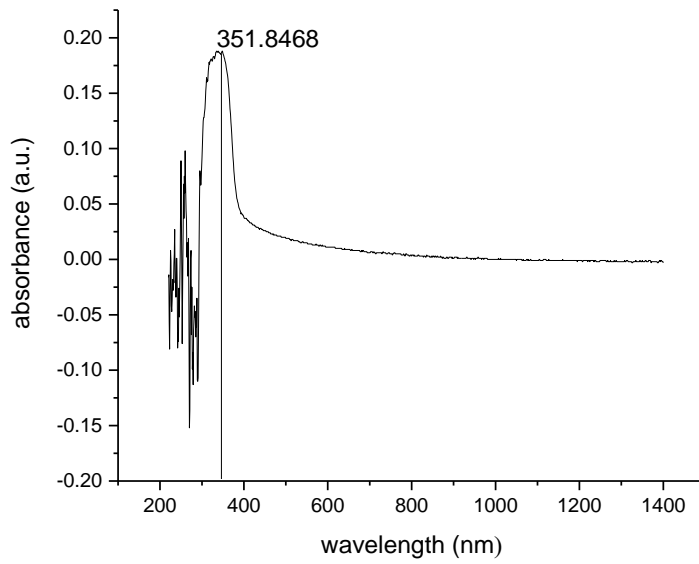


Figure 4. 23. UV spectrum of ZnO film with spin speed of 2000 rpm and annealing temperature of 300 °C.

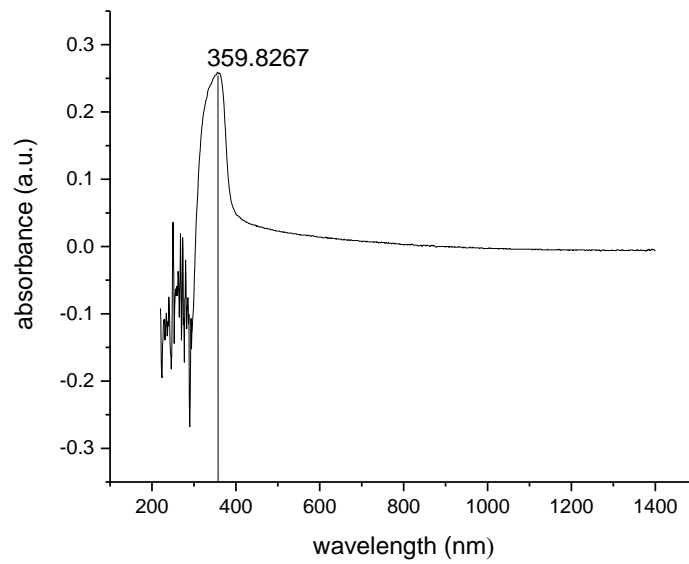


Figure 4. 24. UV spectrum of ZnO film with spin speed of 1500 rpm and annealing temperature of 400 °C.

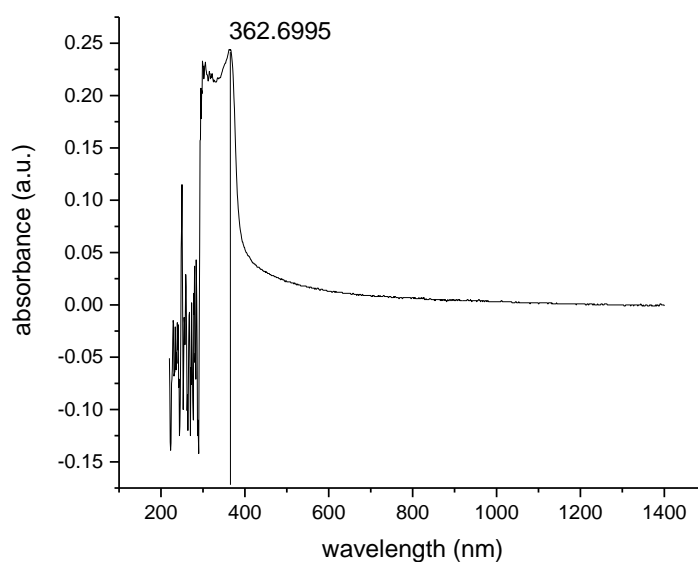


Figure 4. 25. UV spectrum of ZnO film with spin speed of 1500 rpm and annealing temperature of 500 °C.

Table 4. 4

Energy band gap of UV emission peak at different spin speed and annealing temperature of ZnO thin film

Sample	Spin Speed (rpm)	Annealing Temperature (°C)	First Excitonic Peak (nm)	Energy band gap (eV)
A	1000	300	343.5477	3.6109
B	1500	300	348.9740	3.5547
C	2000	300	351.8468	3.5257
D	1500	400	359.8267	3.4475
E	1500	500	362.6995	3.4202

4.3 Piezoelectric Test

The voltage that produced by ZnO thin film was measured for three minutes with fixed frequency of 40 kHz. During piezoelectric test, the voltage produced was inconsistent. Table 4.5 shows the maximum and minimum voltage that each film could produce. The average voltage was calculated by the ratio of voltage which was taken every 10 s to number of reading as shown in Appendice A2.

From the results, it showed when increasing annealing temperature, the voltage produced was increased. When increasing the rotation speed, the voltage produced was increased. The highest voltage was produced by ZnO film with rotation speed of 2000 rpm and annealing temperature of 300 °C. The maximum voltage produced from this film was 27.3 mV, lowest voltage was 0.9 mV and average voltage was 6.353 mV. ZnO film with rotation speed of 1000 rpm and annealing temperature of 300 °C produced the least voltage which was 1.374 mV.

The maximum and minimum voltage that produced by ZnO film with spin speed of 1500 rpm and annealing temperature of 180 °C was 202 mV and 0.142 mV. The average voltage produced was 174 mV. However, the film that produced was not uniform film. The ZnO was accumulated. Therefore, it was believed that the voltage produced could be very high because of the film was thick enough. Figure 4.26 shows the ZnO film with spin speed of 1500 rpm and annealing temperature of 180 °C.



Figure 4. 26. ZnO film with spin speed of 1500 rpm and annealing temperature of 180 °C.

Table 4. 5
Voltage that could be produced by each films

Sample	Spin Speed (rpm)	Annealing Temperature (°C)	Average Voltage (mV)	Minimum Voltage (mV)	Maximum Voltage (mV)
A	1000	300	1.374	0.5	2.4
B	1500	300	1.368	0.9	2.1
C	2000	300	6.353	0.4	27.3
D	1500	400	1.384	0.9	3.5
E	1500	500	1.424	1.1	1.8

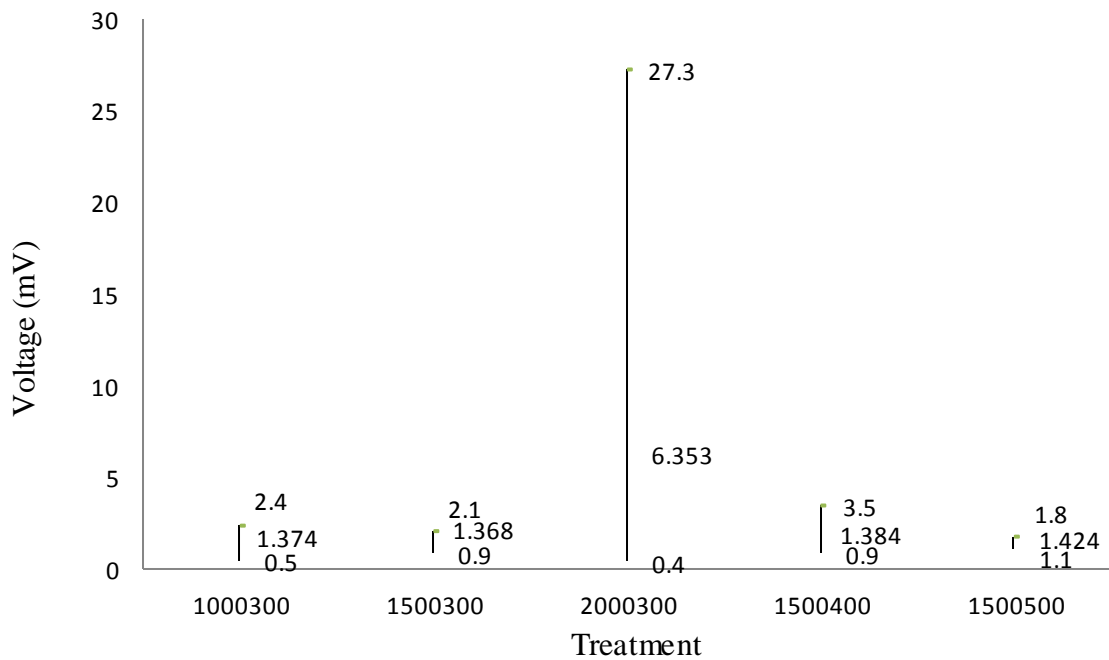


Figure 4. 27. Voltage produced by each film.

CHAPTER 5

CONCLUSION AND RECOMMENDATION

5.1 Conclusion

The objective of this research was to determine the piezoelectric voltage that could be produced by ZnO film. From XRD results, the films were preferentially diffracted at 65° which corresponding to (1 1 2) crystal plane. From the PL results, it was observed that there was only film with spin speed of 2000 rpm and annealing with 300°C had shorter wavelength which is around 380 nm. Piezoelectric test had proven the ZnO film could produce electricity. The maximum voltage (27.3 mV) was produced by the ZnO film with spin speed of 2000 rpm and annealing with 300°C as it has smallest crystallite size, thinnest film and shorter wavelength in PL results. The voltage output is sufficient to become source of energy for some millivolt sensor devices.

5.2 Recommendations

There were some limitation in this research, some recommendations was raised in this section to improve the experiment. The film with spin speed of 1500 rpm and annealing temperature of 180°C was accumulated and could not get uniform film. Dip coating might be used to improve the uniformity of film. One of the limitation in this research was the XRD detection. The films were too thin to be detected by XRD. Therefore, more layers should be coated to be able to detect. The sample preparation is crucial step. A little bit of contaminant will affect the result. Personal Protective Equipment must be worn throughout the entire process. Cleanliness of surrounding must be taken care. Rather than aluminum was used as substrate, ITO glass could be used as

substrate. Besides that, the reading of multimeter in piezoelectric test is inconsistent. Keithley instrument should be used so that the reading could be recorded. The other limitation was the sample could not contact directly with the vibrator, therefore, the vibration produced was too weak to be detected by samples. Other vibrators such as ChromTech Ultrasonic Cleaner could be used to improve the vibration strength.

REFERENCES

- Abdel Aal, A., Mahmoud, S., & Aboul-Gheit, A. (2009). Sol-Gel and Thermally Evaporated Nanostructured Thin ZnO films for Photocatalytic Degradation of Trichlorophenol. *Nanoscale Research Letters*, 627-634.
- Akgun, M. C., Kalay, Y. E., & Unalan, H. E. (2012). Hydrothermal zinc oxide nanowire growth using zinc acetate dihydrate salt. *Material Research*, 1445-1451.
- Alias, S. S., & Mohamad, A. A. (2013). *Synthesis of Zinc Oxide by Sol GEL Method for Photoelectrochemical Cells*. Springer Science & Business Media.
- Aricò, A. S., Bruce, P., Scrosati, B., Tarascon, J.-M., & Schalkwijk, W. v. (2005). Nanostructured materials for advanced energy conversion and storage devices. *Nature Materials*, 4, 366 - 377.
- Bae, H., & Choi, G. (1999). Electrical and reducing gas sensing properties of ZnO and ZnO-CuO thin films fabricated by spin coating method. *Sensors and Actuators B: Chemical*, 47-54.
- Brinker, C., & Scherer, G. (2013). *Sol Gel Science*. San Diego: Academic Press.
- Brus, L.E. (1984). Electron-electron and electron-hole interaction in small semiconductor crystallites: The size dependence of the lowest excited electronic state. *The Journal of Chemical Physics*, 4403-4409.
- Chen, J., He, S., & Sun, Y. (2014). *Rechargeable Sensor Networks: Technology, Theory, and Application: Introducing Energy Harvesting to Sensor Networks*. Singapore: World Scientific.
- Concept of energy harvesting*. (n.d.). Retrieved November 23, 2016, from Ambiosystems LLC.: <http://www.ambiosystems.com/index.php/2-uncategorised/13-concept-of-energy-harvesting>
- E.Heredia, Bojorge, C., CAsanova, J., Canapa, H., Craievich, A., & Kellermann, G. (2014). Nanostrucute ZnO thin films prepared by sol-gel spin-coating. *Applied Surface Science*, 317, 19-25.
- Eom, C.-B., & Trolier-Mckinsty, S. (2012). Thin-Film piezoelectric MEMS. *MRS Bulletin*, 1007-1017.
- Gattorno, G., & Oskam, G. (2006). Forced hydrolysis vs self-hydrolysis of zinc acetate in ethanol and iso-butanol. *The Electrochemical Society* (pp. 23-28). ECS.
- Habibi, M. H., & Sardashti, M. K. (2008). Structure and morphology of nanostructured zinc oxide thin films prepared by dip- vs. spin-coating methods. *Iranian Chemical Society*, 5(4), 603-609.
- Joshi, S., Nayak, M., & Rajanna, K. (March 2014). Effect of post-deposition annealing on transverse piezoelectric coefficient and vibration sensing performance of ZnO thin films. *Applied Surface Science*, 296, 169-176.

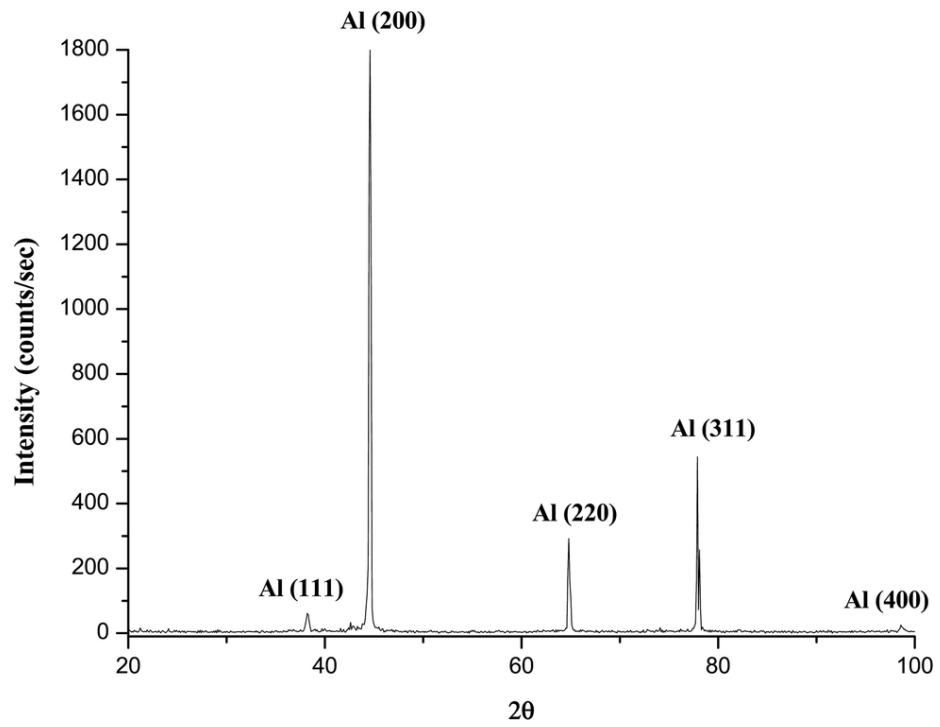
- Khaligh, A., Zeng, P., & Zheng, C. (2010). Kinetic energy harvesting using piezoelectric and electromagnetic technologies-state of the art. *IEEE Transactions on Industrial Electronic*, 57(3), 850-860.
- Kondraties, V., Kink, I., & Romanov, A. (2013). Low temperature sol gel technique for processing Al-doped zinc oxide films. *Material Physics and Mechanics* 17, 38-46.
- Kumar, B., & Kim, S.-W. (2012). Energy harvesting based on semiconducting piezoelectric ZnO nanostructures. *Nano energy*, 1(3), 342-355.
- Kumar, N., Kaur, R., & Mehra, R. (2007). Photoluminescence studies in sol-gel derived ZnO film. *Journal of Luminescence* , 784-788.
- Levy, D., & Zayat, M. (2015). *The Sol-Gel Handbook*. John Wiley & Sons.
- Li, Y., Xu, L., Li, X., Shen, X., & Wang, A. (2010). Effect of aging time of ZnO sol on the structural and optical properties of ZnO thin films prepared by sol-gel method. *Applied Surface Science*, 4543-4547.
- Liu, Z., Li, J., Ya, J., Xin, Y., & Jin, Z. (2008). Mechanism and characteristics of porous ZnO films by sol-gel method with PEG template. *Materials Letters*, 1190-1193.
- Manikandan, M., Gopal, J., & Chun, S. (2016). Sonophysical cost effective rapid indigenous preparation of aluminium particles via exfoliation of aluminium foil. *RSC Adv.*, 32405-32413.
- Monk, P., Mortimer, R., & Rosseinsky, D. (2007). *Electrochromism and Electrochromic Devices*. Cambridge University Press.
- Nanda, S., & Gupta, P. (2010). Structural and Optical Properties of Sol-gel Prepared ZnO Thin Film. *Applied Physics Research*, 19-28.
- Natsume, Y., & Sakata, H. (2000). Zinc oxide films prepared by sol-gel spin-coating. *Thin Solid Films*, 30-36.
- Nechibvute, A., Chawanda, A., & Luhanga, P. (2012). Piezoelectric energy harvesting devices: an alternative energy source for wireless sensors. *Smart Materials Research*, 2012.
- Nuffer, J., & Bein, T. (2006). Application of piezoelectric materials in transportation industry.
- P.B., K., Moloto, M., & Sikhwivhilu, L. (2012). The effect of solvents, acetone, water and ethanol, on the morphological and optical properties of ZnO nanoparticle prepared by microwave. *Journal of Nanotechnology*, 1-6.
- Pierre, A. C. (1998). *Introduction to Sol-Gel Processing*. Boston/Dordrecht/London: Kluwer Academic Publishers.

- Prashanthi, K., Miriyala, N., Gaikwad, R., Moussa, W., V.Ra, g. R., & Thundat, T. (2013). Vibrational energy harvesting using photo-patternable piezoelectric nanocomposite cantilevers. *Nano Energy*, 2(5), 923-932.
- Quinones-Galvan, J., Sandoval-Jimenez, I., Tototzintle- Huitle, H., Hernandez-Hernandez, L., de Moure-Flores, F., Compos-Gonzalez, E., . . . Araiza-Ibarra, J. (2013). Effect of precursor solution and annealing temperature on the physical properties of sol-gel deposited ZnO thin films. *Results in Physics*, 248-253.
- Sagar, P., Kumar, M., Mehra, R., Okada, H., Wakahara, A., & Yoshida, A. (2007). Epitaxial growth of zinc oxide thin films on epi-GaN/sapphire (0001) by sol-gel technique. *Thin Solid Films*, 3330-3334.
- Sagar, P., Shishodia, P., Mehra, R., Okada, H., Wakahara, A., & Yoshida, A. (2007). Photoluminescence and absorption in sol-gel-derived ZnO films. *Journal of Luminescence*, 800-806.
- Sahu, N., Parija, B., & Panigrahi, S. (2009). Fundamental understanding and modeling of spin coating process: A review. *Indian Journal of Physics*, 493-502.
- Sazonov, E., Li, H., Curry, D., & Pillay, P. (2009). Self-powered sensors for monitoring of highway bridges. *Sensors Journal*, 1422-1429.
- Schodek, D. L., Ferreira, P., & Ashby, M. F. (2009). *Nanomaterial, Nanotechnologies and Design*. Butterworth-Heinemann.
- Schweizer, P. M., & Kistler, S. F. (2012). *Liquid film coating: scientific principles and their technological implications*. Springer Science & Business Media.
- Shang, Z., Li, D., Wen, Z., & Zhao, X. (2013). The fabrication of vibration energy harvester arrays based on AlN piezoelectric film. *Journal of Semiconductor*, 34(11), 114013.
- Shivaraj, B. W., Murthy, H. N., Krishna, M., & Satyanarayana, B. S. (2015). Effect of annealing temperature on structural and optical properties of dip and spin coated ZnO thin films. *Procedia Materials Science*, 10, 292-300.
- Spies, P., Pollak, M., & Mateu, L. (2015). *Handbook of energy harvesting power supplies and application*. CRC Press.
- Ville, K. (2010). Microstructured piezoelectric shoe power generator outperforms batteries. *MEMS Investor Journal*.
- Vives, A. A. (2008). *Piezoelectric Transducers and Application*. Springer Science & Business Media.
- Wang, M., Kim, E., Chun, J., Shin, E., Hahn, S., Lee, K., & Park, C. (2006). Influence of annealing temperature on the structure and optical properties of sol-gel prepared ZnO thin film. *Physica Status Solidi (a)*, 2418-2425.
- Wang, Z. L., & Wu, W. Z. (2014). Piezotronics and piezo-phototronics: fundamentals and applications. *National Science Review*, 1(1), 62-90.

- Wang, Zhong Lin. (2004). Zinc oxide nanostructures: growth, properties and application. *Journal of Physics: Condensed Matter*, R829-R858.
- Wong, H., & Dahari, Z. (2015). Human body parts heat energy harvesting using thermoelectric module. *Energy Conversion (CENCON)* (pp. 211-214). IEEE.
- Wu, T., & Thompson, D. (2010). The vibration behavior of railway track at high frequencies under multiple preloads and wheel interactions. *Journal Acoust Soc. A.*, 1046-1053.
- Xu, L., Zheng, G., Lai, M., & Pei, S. (2014). Annealing impact on the structural and photoluminescence properties of ZnO thin films on Ag substrate. *Journal of Alloys and Compounds*, 560-565.
- Yahya, N. (2011). *Carbon and oxide nanostructures: synthesis, characterisation and application*. Springer Science & Business Media.
- Yu, W. W., Qu, L., Guo, W., & Peng, X. (2003). Experimental determination of the extinction coefficient of CdTe, CdSe and CdS nanocrystals. *Chemistry of Materials*, 2854-2860.
- Zhu, M., Xia, J., Hong, R., Abu-Samra, H., Huang, H., Staedler, T., . . . Jiang, X. (2008). Heat-activated structural evolution of sol-gel-derived ZnO thin films. *Journal of Crystal Growth*, 816-823.
- Znaidi, L. (2010). Sol-gel-deposited ZnO thin films: A review. *Material Science and Engineering: B*, 18-30.

APPENDICES A1

XRD SPECTRUM OF PURE ALUMINUM



Source: Reproduced from (Manikandan, Gopal, & Chun, 2016)

APPENDICES A2

MEASUREMENT OF PIEZOELECTRIC TEST

time (s)	Voltage (mV)				
	1000300	1500300	2000300	1500400	1500500
0	1.2	1.3	3.2	1.2	1.3
10	1.4	1.6	3.3	1.3	1.7
20	1.3	1.5	3.4	1.4	1.5
30	0.7	1.4	3.2	1.3	1.3
40	1.6	1.3	7.8	1.7	1.4
50	1.4	1.3	20.5	3.5	1.3
60	1.4	1.6	11.6	1.3	1.4
70	1.4	1.4	3.7	1.4	1.6
80	0.9	1.4	2.3	1.3	1.3
90	2.4	1.3	2.3	1.2	1.8
100	1.4	1.3	5.6	1.3	1.3
110	1.5	0.9	2.9	1.5	1.4
120	1.3	1.2	15.7	1.2	1.5
130	1.4	2.1	27.3	1.1	1.3
140	1.3	1.2	4	1.6	1.6
150	1.8	1.2	1.7	1	1.1
160	1.7	1.2	0.8	1	1.1
170	0.5	1.3	1	1.1	1.65
180	1.5	1.5	0.4	0.9	1.5
total	26.1	26	120.7	26.3	27.05
average	1.373684	1.368421	6.352632	1.384211	1.423684